# Seismic Depth Imaging of Complex Structures

*An example from Zagros fold and thrust belt, Iran*

**Behzad Alaei**


Dissertation for the degree philosophiae doctor (PhD)

at the University of Bergen

2006

# Preface

This thesis is the result of three years research on seismic depth imaging of complex structures of thrust and fold belts with example from the Iranian Zagros fold belt. I left National Iranian Oil Company after more than 10 years of working to the University of Bergen in order to strengthen my scientific background in one of the subjects that is a hot topic in the exploration seismology.

The thesis is organized according to the regulations of the University of Bergen and consists of two separate and complementary parts:

Part I: Monograph or summary that includes 7 chapters and 64 pages. This part includes a summary of the research results presented in the papers in part II, and is meant to provide the overview of the entire research conducted and the relations between the papers. In this sense there is inevitably some repetitions between part I and II, however there is also additional information and some elaborations on the individual results that are presented in the papers in part II.

In the first chapter (Introduction) the objectives of the thesis, seismic imaging problems in complex structures of thrust and fold belts with special reference to Zagros fold belt and the state of the art solution presented. This chapter continued with a brief summary of the geologic setting of the Zagros fold belt and the data specifications (a regional 2D time migrated seismic line and a 3D preprocessed time gathers from mountainous area in the Zagros fold belt) used in this research.

The second chapter is about the 2D regional asymptotic interface based modeling (first paper of part II) in the Zagros fold belt. This is for the first time that seismic forward modeling has been applied in the Zagros fold belt.

The third chapter is a short but necessary section about additional pre-processing for seismic depth imaging purposes especially in areas of poor quality reflection seismic data.
The fourth chapter includes the proposed procedure for depth migration velocity analysis using tomographic updates (the second paper of part II) constrained with different a priori information. The procedure has been applied on a 3D dataset from Zagros fold belt and the results also briefly presented in this chapter.

The fifth chapter is about single arrival Kirchhoff prestack depth migration (The third paper of part II). In this chapter the results of 4 different single arrival Kirchhoff prestack depth migration is presented.

In the sixth chapter the effect of detailed modelling in complex structures has been investigated (The fourth paper of part II). The complexity of seismic wavefield has been revealed with detailed geological modelling of the overburden and target intervals. Finite difference forward realization has been used at this part of the research.
The seventh (last) chapter is the conclusion. This includes the concluding remarks for the whole research.

Part II: This part consists of the four papers out of which three are already published in relevant scientific journals and the fourth one is in peer-review. Following is a list summarizing the state of each paper.

Paper 1: Alaei, B., 2005. Seismic forward modelling of two fault-related folds from the Dezful embayment of the Iranian Zagros Mountains. Journal of seismic exploration, vol. 14, Number 1, 13-30.

Paper 2: Alaei, B., 2005. An Integrated procedure for Migration Velocity Analysis in complex Structures of thrust- belts. Journal of Applied Geophysics xx (2005) xxx–xxx (available online from December 20, 2005).

Paper 3: Alaei, B., and J., Pajchel, 2006. Single Arrival Kirchhoff prestack depth migration of complex structures from Zagros fold belt. CSEG Recorder vol. 31, January 2006, pp 41-48.

Paper 4: Alaei, B., and S., A., Petersen. Detail geological modelling and finite difference forward realization of a regional section from the Zagros fold belt (Submitted to The Petroleum Geoscience).

Page numbers are continuous for part I however for part two they are different, where the page numbers of the first three papers are the numbers assigned by the journals

Most of the figures presented in part I do not have their exact locations. This is due to the limitations posed by the confidentiality of the data used in this research which is in accordance with the terms and conditions stated in the confidentiality agreement that has been signed between the institute and the Oil Company. Although the exact locations of the seismic lines are not shown (i.e. the horizontal axes information is either too small to read or not shown), the horizontal scale is indicated by a scale bar allowing the reader to understand the lateral extent.

Behzad Alaei

January 31, 2006

# Contents

## Part II papers

Paper 1: Alaei, B., 2005. Seismic forward modelling of two fault-related folds from the Dezful embayment of the Iranian Zagros Mountains. Journal of seismic exploration, vol. 14, Number1, 13-30.

Paper 2: Alaei, B., 2005. An Integrated procedure for Migration Velocity Analysis in complex Structures of thrust- belts. Journal of Applied Geophysics xx (2005) xxx–xxx (available online from December 20, 2005).

Paper 3: Alaei, B., and J., Pajchel, 2006. Single Arrival Kirchhoff prestack depth migration of complex structures from Zagros fold belt, CSEG Recorder, vol. 31, January 2006, pp 41-48.

Paper 4: Alaei, B., and S., A., Petersen. Detail geological modelling and finite difference forward realization of a regional section from the Zagros fold belt (Submitted to The Petroleum Geoscience).

# Acknowledgments

I am grateful to several people for their help and guidance. I thank my supervisor, Professor Kuvvet Atakan, not only for his supervision but also for his organized and continuous support.

I thank my parents, from whom I learned the values of hard work. They had a great attention to their children's education and I am grateful for that.

I am grateful to the University of Bergen, Department of Earth Science. Without their support I could not have completed this thesis. I thank the institute's staff for their friendly cooperation. They made my life at Bergen much easier than it could have been. I am a grateful beneficiary of their kindness and generous support.

I would like to thank the great teachers I had growing up, particularly, Dr. Eliasi from department of Geology of Tehran University, Dr. Gheitanchi from Geophysics institute of Tehran University, Profess Tore Arne Johansen, Leif Bruland, and William Helland-Hansen from the University of Bergen. Special thanks to Dr. Rowhani from Tehran University who showed me how interesting science and particularly physics could be and Professor Einar Maland from the University of Bergen for showing me the mathematics and many invaluable facts about seismic data processing.

National Iranian Oil Company (NIOC), exploration directorate has provided the whole dataset for this thesis. I appreciate their friendly cooperation particularly from Geophysics department. Special thanks to Mr. Mohadess, Zad Mohammadi, Khorasani, and Naini. The support of my friend Hamid Zandifar was considerable. I appreciate all his kind support. My friends at the university of Bergen, Mohammad Raeesi, and Pourdad Farzadi are highly appreciated. I would also like to thank Dr. Mohammad Mokhtari for his help.

I would like to thank Norsk Hydro for their financial support. I have benefited from the facilities provided at the Norsk Hydro's research centre in Bergen. They have provided all necessary resources including powerful computer facilities, and software and helped me through the research. I appreciate the kind help from all staff at the research centre. I will never forget their excellent cooperation. Special thanks to Gro Haatvedt, Per Riste, Arne Rasmussen, Dave Hunt, Dimitri Lokshtanov, Stig-Morten Knutsen, and Ridvan Karpuz. Special thanks to Steen Petersen, for his great help in forward modelling and the idea of shared earth modelling. Special thanks to Brian Farrelly who has done the difficult task of language improving of my writings. Jan Pajchel's advice from the beginning of the thesis was excellent. He showed me new horizons and

exciting ideas and gave me the confidence to work. I appreciate his invaluable expertise in seismic exploration and all his support. Without his help I could have never completed this thesis. I thank Mr. K. Odouli for his very good and valuable advises. Finally I want to thank my wife, Anita. Her patience, love, and support gave me the strength to complete this work. She always supports me and encourages me to move forward. There are no words to express how happy and grateful I am to have her by my side. I dedicate my thesis to her for her great support. I would like to thank so much from my children, my dear son, Armin and my little daughter, Arezo for their understanding during my PhD.

## Abstract

The ultimate goal of seismic data processing is to recover an image of the subsurface geological structure. Seismic forward modelling has been applied in a regional 2D section from the Zagros Fold and Thrust belt (FTB) in order to evaluate the seismic response and quantify the imaging problems in the Zagros type setting. Both asymptotic and finite difference forward realization methods have been applied. The shared earth modelling strategy has been used in the model building process for finite difference realization. The method represents the subsurface independent of the input requirements of the forward algorithms. The structural and stratigraphic detail included in the model is completely consistent with the real geological details. The finite difference seismic response shows several non-hyperbolic events, and diffractions. Poor illumination occurs under the thrust fault planes and thick overburden (salt and shale units).

In areas of complex geology, such as subsalt structures or fold thrust belts (for example Zagros FTB), prestack depth imaging is the only way to produce an accurate image of the subsurface. Seismic depth imaging includes velocity estimation and migration. Velocities are needed for depth migration, the process that converts seismic data, recorded as functions of time, into a depth image of the subsurface.

Conventional velocity analysis methods generally assume flat-layered geology with small lateral velocity variations. In areas of complex geology, the velocity structure is correspondingly complex, with significant lateral variations, so conventional velocity estimation methods fail, and more sophisticated techniques are required. One of these methods, seismic reflection tomography, compares observed traveltimes, measured for each source-receiver, with modelled traveltimes computed by ray tracing through a pre-defined velocity model. The differences are projected back over the traced ray paths to generate the updated velocity model. Reflection tomography often converges slowly. When pre-stack depth migration is performed with incorrect velocity model reflectors in depth migrated gathers are not flat. The degree of non-flatness is a measurement of the error in the model. Tomography uses this measurement of non-flatness (residual moveout) as input and attempts to find an alternative model, which will minimize the errors. One of the most common and also practical ways to constrain the velocity determination process is through seismic interpretation. Velocity model building is far more effective when strongly linked to an interpreted structure. An interpretational velocity analysis approach in seismic exploration ensures the development of accurate results.

An integrated velocity estimation method based on hybrid tomographic methods (grid-based and layer-based) is presented for a complex structure. In the proposed workflow, seismic

interpretation and geological controls are involved in the tomographic interval velocity analysis from the very first stage of initial model building up to the final updated high-resolution velocity model. The integrated method has been applied on a real 3D dataset from the Iranian Zagros FTB. This is significant because of the paucity of published processing examples for the complex overthrust and mixed carbonate-clastic-evaporate typical of the Zagros setting. The final velocity obtained improves to a large extent the focusing of the migrated image.

Strong topographic variations, and irregular spatial sampling in the Zagros, make the Kirchhoff prestack depth migration the method of choice. Single arrival Kirchhoff prestack depth migration method has been applied to the 3D dataset from mountainous area of the Zagros. Both minimum travel time and shortest path have been tested as criteria for the single arrival. Two different coordinate systems (rectangular and spherical) have been used in computing the travel times. The complex velocity structure of the overburden, intense faulting, significant thickness variation and folds with steep to overturned flanks were among the sources of complexity in the area. Around the flanks of folds with very steep limbs the single arrival with the shortest path and not the minimum travel time, gives better focusing. The spherical coordinate system for travel time computation gives better results.

# Part I Summary

# 1 Introduction

## 1.1 Objectives of the thesis

The ultimate goal of seismic data processing is to recover an image of the subsurface geological structure. Seismic imaging in general and seismic depth imaging in particular is the most computationally demanding part of seismic processing. Seismic depth imaging includes velocity estimation and migration as the two parts that are closely linked together. Velocity is needed in order to have proper focusing of the data during migration and migration itself removes the effects of the wave propagation from source to imaging point and back to the receiver. In complex geological situations such as subsalt structures or fold and thrust belts seismic depth imaging becomes difficult from the point of view of velocity estimation and of migration. Fold and thrust belts are an integral part of the orogenic belts in the world that have received great attention due to their high potential for hydrocarbon exploration. Therefore exploration seismologists have intensively investigated seismic depth imaging of these folds and thrust belts.

The first oil discovery in Iran occurred on May 26th 1908 in Masjide Soliman in Asmari carbonates of the Iranian Zagros FTB. The first seismic refraction acquisition was acquired in the late 1920's in the Zagros area and continued later by reflection methods. Structural complexities in the studied area were first seen in the late1940's. For instance in Lali 11 some repeated intervals were observed and has been interpreted as reverse faulting in 1948 (Motiei, 1995). Later the structural complexities became more evident since the simple structural traps-anticlines, had already been explored. Reflection seismic data were quite useful in finding the crestal parts of structural traps but in most of the discovered oil fields the 2D high coverage seismic profiles failed to give a good and clear image from the flanks of the structures (particularly the southern one). This ambiguity in the structural definition made the interpretation difficult and more dependent on knowledge of structural styles (Bally, 1983, Mitra and Fisher, 1992). The reliance on structural styles is necessary in view of the fact that the quality of the seismic images of fold and thrust structures is poor. Parts of the stratal geometry maybe clearly shown while other parts show either a lack or a confusing overabundance of reflection signals (Lingrey, 1991). Figure 1.1 shows one example of the ambiguity in seismic images from the structures in the Zagros FTB. The northeast flank can easily be interpreted while the continuation of the structure towards the southwest is not clear. Therefore complexities in the structure are one of the main sources of the reduction in seismic image quality. So I had the question in mind,

***" Is there any possibility of improving the quality of the images to obtain a better understanding of the subsurface by seismic depth imaging?"***

The sources of complexities are not sources of noise but they can be regarded as sources of our failure in data analysis. As Jon Claerbout (1985) has stated: “Noise in seismology can usually be regarded as a failure of analysis rather than something polluting the data “. So the main objective of this study is 3D seismic depth imaging of complex structures with an integrated approach. This includes forward modelling, depth migration velocity analysis, and prestack depth migration. The two parts of the seismic depth imaging- velocity estimation and migration will be looked at in detail in an integrated approach. The idea is to investigate the currently available methods in seismic depth imaging and combine them with the complexities explained above to derive a solution for seismic imaging in the Zagros FTB.

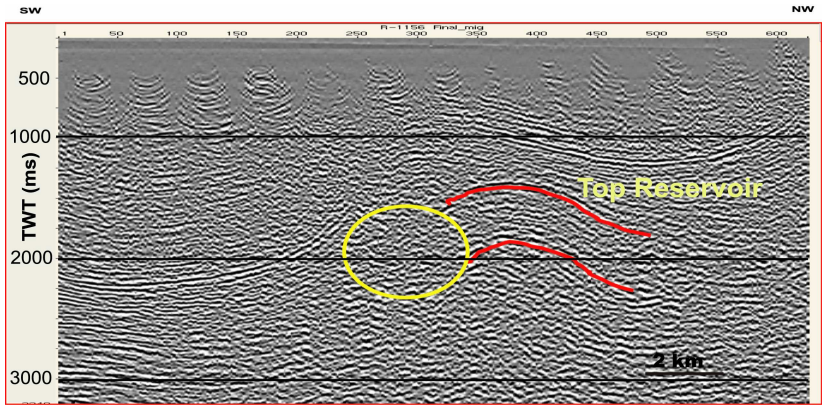


*Figure 1.1 2D migrated seismic profile (1200% coverage) from the Dezful embayment area. The seismic image quality in one flank of almost all of the structures (usually the southern flank) is poor. The yellow ellipse shows the complex flank.*

## 1.2 Imaging Problems in Zagros FTB

Most of the problems in seismic imaging are due to the complexities of fold thrust belts both in structure (structure dependent complexities) and rock types (structure independent). Figure 1.2 is a sketch cross-section through a typical thrust and fold belt from Jones, (1982). Some of the difficulties in fold and thrust belts are: steep dip of the beds, overturned beds, complex thrust fault geometry (along the bedding planes and cutting the beds), detachment levels, thrust vergence, repeated intervals, and asymmetric folds associated with thrusts. It is the task of seismic imaging in thrust and fold belts to reveal these types of structural complexities in seismic reflection data.

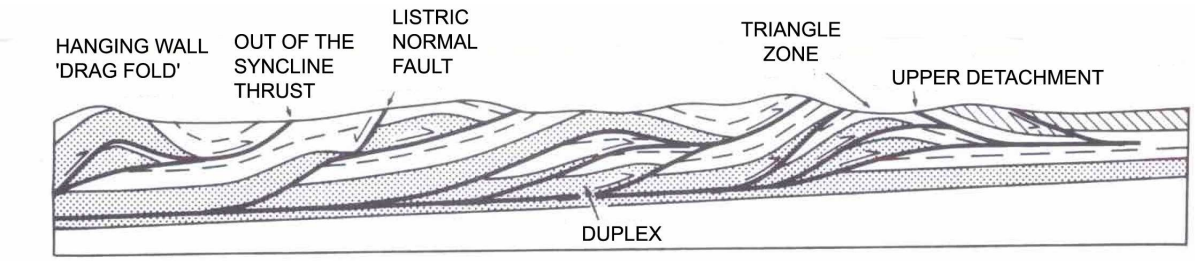


*Figure 1.2 Typical thrust belt, showing thrust and listric normal faults, duplex structures, and underthrust foreland margin (Jones, 1982).*

In the Zagros FTB these problems exists together with difficulties associated with a variable thickness, incompetent, internally faulted and folded shallow section which is deformed in a disharmonic style with respect to the deeper section. The complexities in the Zagros FTB can be summarized as follows:

There are two mega intervals in the Zagros FTB (Figure 1.3). The first one (shallow section) is consists of incompetent materials such as marl and salt and it will be called post-Asmari interval (it includes from top Aghajari, Mishan and Gachsaran formations). The second interval (deep section) is consists of competent materials mainly carbonates and will be called pre-Asmari interval. The velocity variation of the two formations above Gachsaran in the post-Asmari interval (Mishan and Aghajari) is more or less depth dependent.

In the lower part of the post-Asmari section (Gachsaran formation right above the Asmari) there is large thickness variation over short distances with internal faulting and folding. This interval shows disharmonic deformation with the pre-Asmari interval. This thickness variation causes

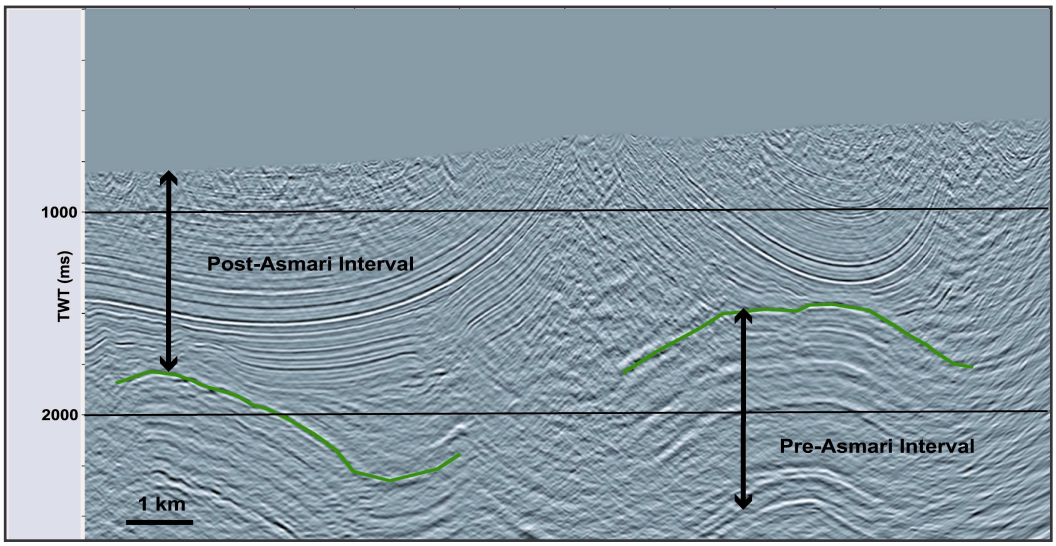


*Figure 1.3 3D prestack time migrated section showing the significant thickness variation in the post-Asmari interval. The interval between the green horizon (Asmari formation) and the surface represents the overburden interval.*

rapid lateral velocity variation that is a challenge for most imaging methods. Internal faulting and folding form a complex geometry that causes severe problems for ray-based imaging methods. Figure 1.3 is a prestack time migrated seismic section that shows the thickness variation of the post-Asmari interval together with its structurally complex geometry (steep dips) The Gachsaran formation includes several layers of salt and anhydrite. The thickness of these salt intervals and of other incompetent intervals changes rapidly due to compression. There are also rapid lateral changes in rock types (due to the nature of deposition of these sediments) making this formation complex in terms of rock properties. There are several velocity inversions in the Gachsaran interval that make it difficult to obtain correct images especially when working with average velocities.

Another problem generated by the Gachsaran formation is poor illumination of the intervals below. This happens particularly when the upper part of the formation is exposed at the surface. In such cases shots are located on this formation and experience has shown that there is a problem with energy penetration to deeper intervals. In these locations obtaining well-focused seismic data is very difficult due to poor illumination. In the Pre-Asmari interval the problems can be summarized as follows:
Fold geometry: In the folds imaging the flanks is almost always a problem especially when the limbs have high dips. In such cases the ray-based imaging methods have difficulties in illuminating the flanks. Good offset distribution is a key factor in imaging
these structures. In the Zagros FTB the flanks of the anticlines in the pre-Asmari interval are usually asymmetric. The unclear image from steep folds became the subject of discussion among geophysicists and geologists. Geophysicists put thrust in the flank of the folds to describe the geometry while geologists believed in overturned limbs of the folds (Motiei, 1995).

The second main problem is the complex internal microstructure of folds in the pre-Asmari interval. Seismic data shows very roughly that the structural configuration of deeper levels in the pre-Asmari interval often conflicts with that defined at shallower parts. As a result of this ambiguity the wells drilled at apparently undisturbed parts of the anticlines (mainly crest of the folds) encountered structural complexity at deeper levels. In such cases any attempt to interpret the poor quality seismic profiles were based mainly on the structural styles not on what can be extracted from the data itself.

The third problem is the effect of major structural elements (so-called basement trends). This type of structures is quite important in terms of geology. Since these elements bring different types of rock units adjacent to each other they cause raypath bending and therefore it is not easy

to follow them in seismic data. The focusing around these structures is a difficult task. The important characteristic feature of these elements is their large vertical extent and limited lateral extent.

The last problem of pre-Asmari interval is lithological variation within rock units. Velocity variation in carbonates is not depth dependent but it is dependent on depositional environment. Therefore it is difficult to derive a correct interval velocity for processing purposes. Velocity inversion also happens in shale units bounded between carbonate units. There are two such major velocity inversions in the pre-Asmari interval.

## 1.3 State of the art solutions

Understanding the complexities of the subsurface is a key factor in selecting the best strategy for seismic imaging. The other important aspect is to understand the limitations of the seismic data that is being imaged. The parameters of the input seismic data including sampling of the data, noise content, and pre-processing steps applied have a severe effect on the results of any seismic depth imaging. In particular understanding the limitations on resolving dip and velocity due to sampling is a key factor (Lines, et al., 2000). The State-of-the-art technology for velocity estimation is global tomographic methods that give structurally consistent results.

Reflection tomography (Stork and Clayton, 1991, Stork, 1992, Clapp, et al., 2004, Van Trier, 1990, Etgen, 1990) is one of the most effective and widely used velocity estimation methods. This is the best way to take into account the lateral variations of interval velocity as opposed to single station velocity analysis methods where any estimation is independent of surrounding points.

Tomography of Common Reflection Point gathers is a method for refining the velocity - depth model when prestack depth migration is performed with an incorrect velocity model. Tomography uses the non-flatness measure of CRP gathers as input and searches for an alternative model, which will minimize the error. There are two methods available for reflection tomography called grid-based (Stork, 1992) and horizon-based (Kosloff, et al., 1996).

There is no more important tool for a structural geophysicist than prestack depth imaging (Lines, et al., 2000). The current state-of-the-art in the migration part of seismic imaging uses wave-equation prestack depth migration for the depth migration algorithm. With land seismic data with strong topographic variation due to the datum related problems these methods do not work as efficiently as with offshore data. Kirchhoff prestack depth migrations that run directly from

topography (Gray, et al., 1998, Gray and Marfurt, 1995, Lines, et al., 1996) have been successful in complex fold and thrust belts.

The goal of this thesis is first to run forward modelling to see the possible problems of imaging in the studied area. This is an important step since there has been almost no attempt before to quantify the depth imaging problems in the Zagros FTB. Asymptotic and finite difference 2D seismic forward realizations on a regional profile crossing several oil fields with good well control provide the opportunity to make the velocity and density close enough to reality. The modelling results are important in understanding the complexities and choosing the best imaging method both for velocity estimation and migration. The second goal is to investigate migration velocity analysis in this complex fold and thrust belt with special reference to the depth tomographic method. The research will be carried out on a land 3D dataset from the Iranian Zagros Mountains with strong topographic variations. The idea is to estimate and modify the velocity in a sequence of processes with different tomographic methods and control the inversion by appropriate a priori information.

Finally after derivation of a velocity model that yields more focused images single arrival Kirchhoff prestack depth migration will be applied with different travel-time calculation methods. Therefore in brief in this dissertation seismic forward modelling (asymptotic and finite difference), a hybrid tomographic migration velocity analysis and prestack depth migration algorithms will be analyzed for complex fold and thrust belts with strong topographic variations.

## 1.4 Geologic settings

The Zagros FTB is located in the south-southwest of Iran and forms the northern edge of the Arabian Plate trending NNW-SSE (Sepehr and Cosgrov, 2004, Sherkati and Letouzey, 2004). Northward movement of the Arabian plate accounts for the crustal shortening in the Zagros with its associated folding, thrusting, and large-scale strike-slip faulting (Sepehr, 2000). Figure 1.4 shows the structural setting and tectonic sub-divisions of the Zagros FTB. Three major deformation fronts are shown in the figure. The regional structural elements bounding the major deformation fronts are the Zagros Main Thrust Fault in the northern part, then the High Zagros Fault, the Mountain Front Fault and finally the Zagros Front Fault in the south. The main tectonic units are the Thrust zone or Imbricate Zone and the Simply Folded Belt (Figure 1.4). In addition to the tectonic division parallel to the mountain belt, the Zagros FTB has some structural trends laterally dividing the whole mountain belt into geological provinces (Sepehr, 2000). These geological provinces from northwest are the Lurestan, the Dezful embayment and the Fars region (Figure 1.4). The Thrust Zone is between the Zagros Main Thrust and High Zagros Fault. Intense

faulting happened in this zone and the geological formations are heavily thrusted in a southwest trend. The Simply Folded Belt is characterized by relatively less intense tectonics. The intensity of folding varies from place to place and most of the folds are almost asymmetrical or overturned and/or overthrust to the southwest.

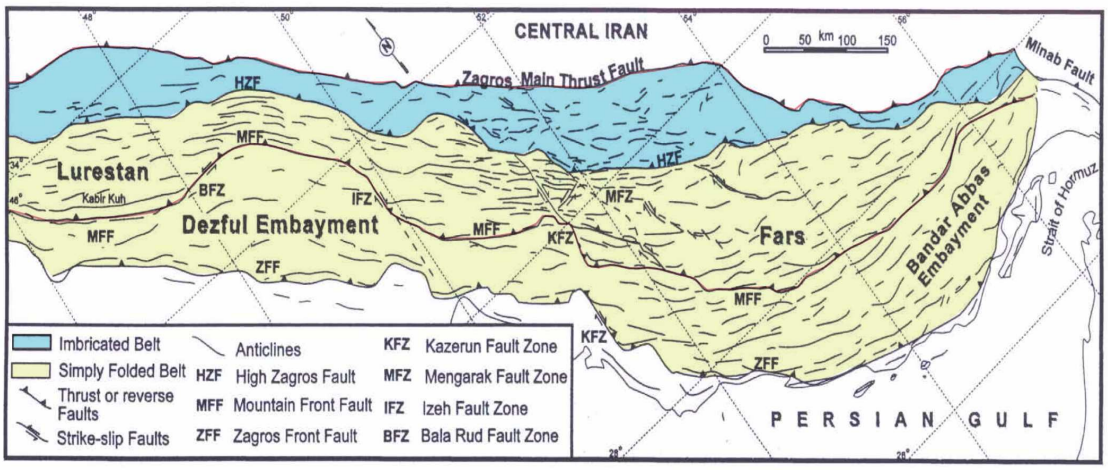


*Figure 1.4 Structural setting and tectonic sub-divisions of the Zagros FTB. The three major deformation fronts of the Zagros and their intersection with strike-slip fault zones are shown in the figure (Sepehr, 2000).*

The morphotectonic subdivisions that are mentioned for the Zagros FTB could be compared with other fold and thrust belts such as the southern Rockies. The foothills, middle range and main western range of the southern Rockies (Mitra, 1992) can be compared with the foothills and Simply Folded Belt and the Thrust Zone in the Zagros FTB. This comparison is good that it can provide some further evidences for subsurface interpretation. The Dezful embayment in the northern part of the Zagros FTB is a structural depression that is characterized by having only two outcrops of the Oligo-Miocene Asmari formation and is one of the geologic provinces inside the Simply Folded Belt that is the transitional zone between Thrust Zone in the north and more stable Khuzestan plain in the south that has experienced varying sedimentation through geological time (Patinson and Takin, 1971, Motiei, 1995). Some geologists (e.g. Favre, 1975) have thought that the style of folding in the Dezful embayment is more or less similar to the northern part of the mountain front and it is always not easy to distinguish the folds from two sides while others (e.g. Mapstone, 1978) have observed a distinct change in structural style across the mountain front fault. Northeast of the Mountain Front Fault structures are tight while southwest of the Mountain Front Fault in the Dezful embayment structures are normally open thrust faulted anticlines with obtuse interlimb angles widely spaced between sub horizontal planar synforms (Mapstone, 1978).

The compressional folding commenced during or soon after the deposition of the Asmari formation. Evidence suggests that the Gachsaran formation was mainly deposited in the subsiding lows in such a way that the thickness variation of this formation is controlled both by deposition

and tectonics (e.g. Oswald, 1978). In late Pliocene times low angle thrusting together with folding had taken place to give a deep structural configuration very much as observed today (Mapstone, 1978).

## 1.5 Data, parameters, complexities

Two different types of data have been used for this research, seismic and non-seismic. The seismic datasets used were both 2D and 3D. The first one is a post stack time migrated 2D seismic line for regional forward modelling purposes and second one is 3D dataset (preprocessed data) from the mountainous area close to the Mountain Front Fault. The location of the 2D seismic line is shown in figure 1.5.

The acquisition and processing parameters of the 2D regional line are listed in table 1:

Table 1: Acquisition parameters of the regional 2D line used in forward modelling

| **RECORDING PARAMETERS** | **RECORDING GEOMETRY** |
|---|---|
| 02-12 to 20-12-1976 | Spread: 0-1080-3900m (0-1200-4020 for shot points 751-803) |
| Format TI DFS V | Station interval: 60m |
| Record Length: 5seconds | Shot point interval: 120m |
| Sampling rate: 2ms | Geophone pattern: 96 geophone G.S.C. 20 D, |
| Filters 8-128Hz | 8 rows of 12 |
| Dynamite reflection surface shooting end on | Shot point pattern: 100LBS (40 charges-4 rows of 10) and 150LBS (60charges –6rows of 10). |

The processing parameters of the 2D regional line are in table 2:

Table 2: processing sequences of the regional 2D line used in forward modelling

| **RECORDING PARAMETERS** | **RECORDING GEOMETRY** |
|---|---|
| 02-12 to 20-12-1976<br>Format TI DFS V<br>Record Length: 5seconds<br>Sampling rate: 2ms<br>Filters 8-128Hz<br>Dynamite reflection surface shooting end on | Spread: 0-1080-3900m (0-1200-4020 for shot points 751-803)<br>Station interval: 60m<br>Shot point interval: 120m<br>Geophone pattern: 96 geophone G.S.C. 20 D,<br>8 rows of 12<br>Shot point pattern: 100LBS (40 charges-4 rows of 10) and 150LBS (60charges –6rows of 10). |

This seismic line has been used during the forward modelling to compare the results with the results of modelling derived data with real data. No processing has been applied on the section in this research. The quality of the 2D seismic line varies from one place to another and from shallow horizons to deeper levels. Elevation varies from about 250m to as high as 1000m along

the line. This is a controlling factor of quality-higher elevation implies less coverage and as a result poor quality. At some parts of the section, reflectors

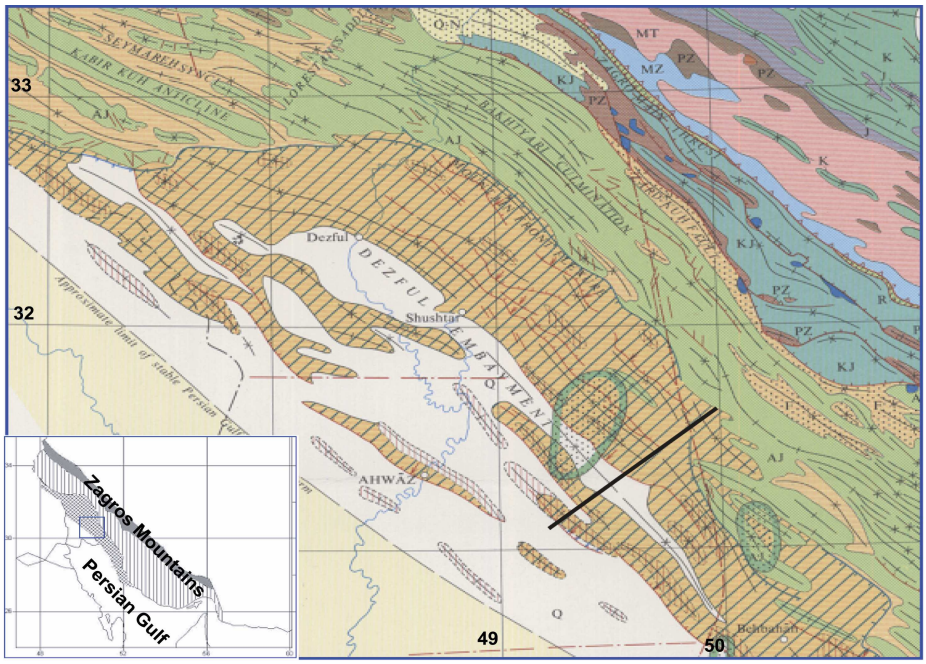


*Figure 1.5 Location map of the regional structural cross section used in forward modelling together with a general stratigraphic table (Huber, 1976).*

can be followed even as deep as 3 seconds but that is only for a small part of the section.I obtained a paper copy of the section. It has been scanned and converted to SEG-Y format by Hampton Data Services (Figure 1.6).The main dataset used is a 3D seismic survey acquired on two producing fields-Parsi and Karanj- located close to the Mountain Front Fault in the Dezful embayment. It is claimed that this is the biggest 3D project in the Middle East (Acquisition report, BGP, 2002). The area is situated in the south west of Iran some 210km southeast of Ahwaz city, one of the Iranian oil industry centres. The nearest city, Behbahan, is located 70 km away to the southeast. The range of the 3D survey is between 49º39'00" E and 50º08'00" E, and between 30º48'00"N and 31º15'00" N. The 3D project is designed with a 40 km length and a width of 20 km, the Receivers cover an area of 792.38 $km^2$ and the shot points cover 779.11 $km^2$. Fig. 1.7 shows the location of the survey area in the Iranian Zagros Mountains. The summary of the acquisition parameters is given in table 3.

The source was explosive with two patterns: pattern (1) 2m X 8Holes X 0.75Kg and pattern (2) 6m X 3Holes X 2Kg. The records quality varies from place to place but generally is poor particularly around Gachsaran outcrops. Figure 1.8 shows an example of the shot records. The instrument parameters is given in table 4.

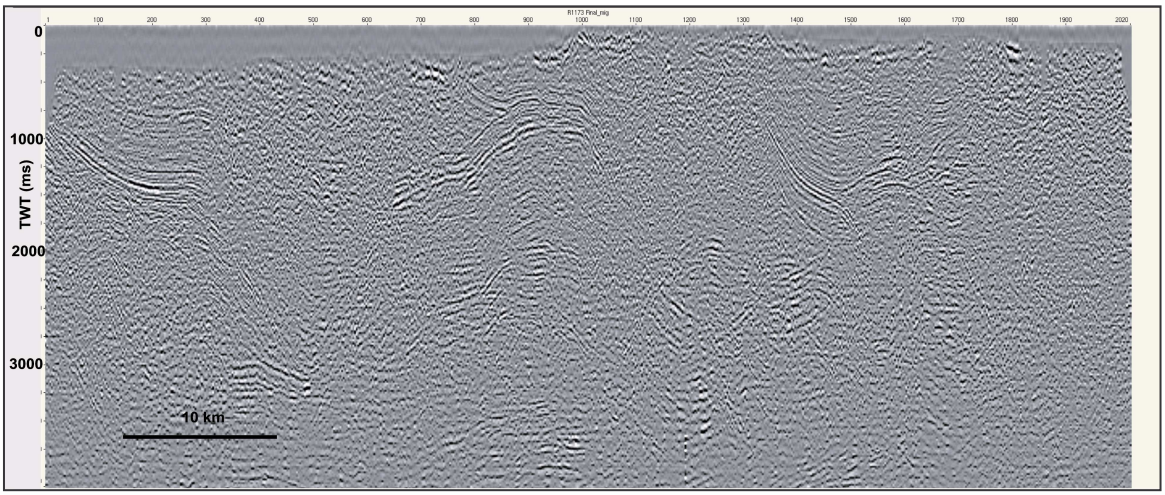


*Figure 1.6 The 2D migrated seismic line (R1173). Data has been recorded and processed by C.F.P.S (1976,1977). The profile includes several faulted anticlines with poor image quality.*

Table 3: The summary of the acquisition parameters of the 3D dataset used in the research.

| Patch parameters | |
|---|---|
| Receiver interval: | 40m |
| Source interval | 80m |
| Receiver line interval | 320m |
| Source line interval | 400m |
| Number of channels per receiver line | 160 |
| Number of channels | 960 |
| Patch | 6 x 160 |
| Number of shots per salvo | 12 |
| Calculated parameters | |
| Bin size | 20m x 40m |
| Full fold | 3 x 8 |
| In-line roll | Rolling 10 stations for one salvo, roll on, roll off |
| X-line roll (after shooting one swath) | Rolling three lines |
| Maximum offset - in line | 3180m |
| Minimum offset - in line | 20m |
| Maximum offset - X line | 1240m |
| Xmax | 3413m |
| Xmin | 465m |
| Aspect Ratio | 0.39 |

Table 4: The instrument parameters of the 3D dataset

| Sampling rate | 2 ms |
|---|---|
| Recording length | 7 sec |
| Preamplifier Gain | 24 dB |
| Notch | Out |
| Low frequency cut | out |
| High Frequency cut | 128 Hz |

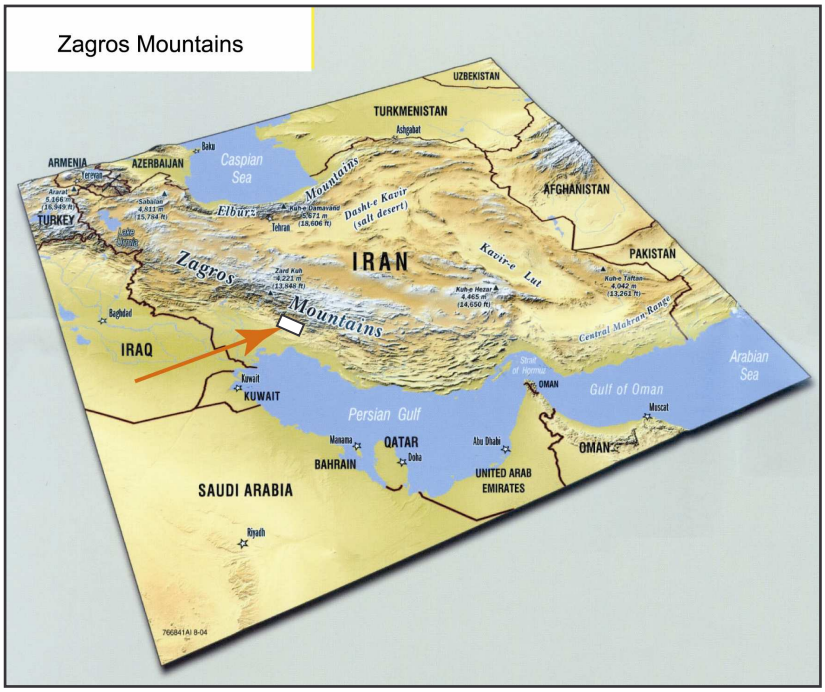


*Figure 1.7 The location of the Parsi and Karanj oil fields in the Dezful embayment of the Zagros FTB.*

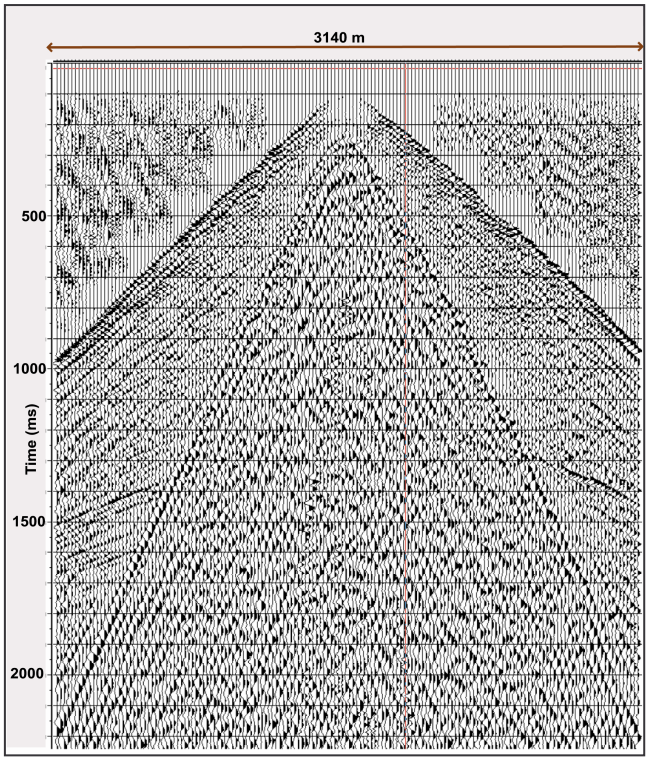


*Figure 1.8 A sample raw shot gather from swath 30 (1 geophone line). The background and ground roll noise is significant (CGG, 2003).*

# 2 Seismic forward modelling (Asymptotic approach) of a regional section from the Dezful embayment of the Zagros FTB

## 2.1 Overview

In mountainous areas, such as the Iranian Zagros FTB, the seismic modelling technique is a valuable tool for seismic acquisition design, processing and reliable interpretation. There are many approaches to seismic modelling. Ray tracing is the one most applicable for structural purposes (Fagin, 1990). However, ray-tracing methods are approximate and they do not take the complete wave field into account.

Structural interpretations of reflection seismic data in foreland fold belts are dependent on structural styles (Bally, 1983, Mitra and Fisher, 1992). The quality of reflection seismic profiles from the Zagros foreland fold thrust belt of southwest Iran, and from other mountain belts (e.g. Canadian Rockies) is typically not good enough to draw the complete configuration of thrusted folds especially in deeper levels. The reliance on structural styles is necessary in view of the fact that the quality of the seismic images of fold and thrust structures is poor. One of the major problems in seismic imaging of fault related folds are revealing the detail internal geometry of the structures. The complexity of the structures may generate wavefield singularities that are not sufficiently accounted for, in standard processing.

A 2D regional cross section (trending northeast-southwest) from the Dezful embayment has been selected. The location of this section is shown in figure 1.5. It crosses four drilled faulted anticlines and extends towards the northeast crossing the Mountain Front Fault. The section has been constructed and balanced by Mapstone, (1978). The section provides a good opportunity to investigate imaging problems in the Zagros FTB because it includes near surface complexities (topographic variations), overburden complexities (thickness variations, strong lateral velocity changes), and reservoir horizon complexities (folds steep flanks, and intensive faulting). It has also several well controls so any forward realization response can be verified based on the direct information from wells.

## 2.2 Model building

The model has been built in two stages: First a regional macro model definition and second a detailed structural model building. The generated section dimension is 81x17 km. It includes 70 interfaces with different lengths and curvatures. Figure 2.1a shows the geometry of the interface-based model. The colour spectrum represents the time processing derived velocity

model. The profile orientation is from southwest (left) to northeast (right), perpendicular to the main structural trend of the Zagros FTB.The selected surfaces are stratigraphic surfaces derived from the drilled wells in the area and structural surfaces representing faults. Faults have been defined as discrete surfaces.

Along with defined geometry, ray-tracing models require the interval velocities between modelled surfaces. There are two sources of velocity data available; processing-derived velocities and well-derived velocities (check shots, vertical seismic profiling data and logs). Therefore two different velocity models have been built. The rectangles in the figure 2.1a show the location of two faulted anticline with doubtful interpretation (Mapstone, 1978). Figure 2.1b and c shows the poststack time- migrated 2D seismic profiles of two faulted anticlines. The two structures have been named 'A' and 'B'. Structure 'A' is Par-e-Siah faulted anticline and structure 'B' is Masjede-e-Soleyman faulted anticline. In Par-e-Siah structure the top reservoir repeated as a result of faulting. The red line in figure 2.1c shows the fault between repeated top reservoir. In Masjede-e-Soleyman faulted anticline the idea is to follow the subthrust (the red line in figure 2.1b) roll over and test the proposed subthrust play by Mapstone, (1978).

## 2.3 Ray tracing results

The seismic response of the regional macro model has been generated and analyzed first. Then the detailed seismic response of the structures 'A' and 'B' have been investigated. Three types of ray tracing modes have been applied including normal incidence, image ray and shot gather ray tracing.

Normal Incidence ray tracing (NIP) is one of the important methods in modelling structural complexities (Sukaramongkol, 1993, Fagin, 1991). It can simulate a CMP stacked section. This is a zero offset mode where the rays have been traced with normal incidence paths with respect to selected interfaces. The travel times of each ray are stored and have been used to generate the stacked unmigrated section. NIP modelling has been applied in a window ($25^{th}$ km to $80^{th}$ km and whole depth range) (Fig. 2.1a) to obtain the stacked unmigrated seismic response of the macro model. Different source-receiver distances have been tested (200, 120 and 60 m). All of the interfaces shown in figure 2.1a have been included in the realization. Missing energy in geometrical and caustic shadows (diffracted rays) has not been accounted for. Figure 2.2 shows the TWT of the interfaces derived from NIP modelling. The continuity of the deep horizons is not preserved. The reflection from the exposed fault around x = 68km (figure 2.1a) has reflections from its plane that extend towards the northeast to 1.5 seconds. The other important horizon is the thrust fault plane coming from the northeast (the ramp part is located between x = 40 km, z = 5

km to x = 55 km, z = 10 km of Figure 2.1a). Understanding the proper configuration of this fault will led us to a better understanding of the structural style. In Figure 2.2, the reflection of the same thrust fault appears between x = 42 km, t = 2.5 s and x = 53 km, t = 5.7 s. This thrust geometry may support the interpretation of fault bend folding style (Suppe, 1983, Mitra and Mount, 1998) for the structure 'B'.

In the next step, zero offset modelling has been applied to structure `A' and `B' separately. At this stage, two types of velocity models have been used in forward realizations. Time processing-derived velocity model and well-derived velocity model. The source-receiver spacing is 60 meters, and for display purposes, the travel times of the rays were convolved with a Ricker zero phase wavelet of 35 Hz. Figure 2.3a and b shows the result of NIP ray-tracing for structures `A', Par-e-Siah faulted anticline. The crestal part of the structure 'A' is not imaged properly (figure 2.3a). The reflector marked as number1 in the figure represents the folded top reservoir and the reflector number 2 is the faulted-repeated top reservoir.

The reflector marked as number 1 in the figure represents the folded top reservoir and the reflector number 2 is the faulted-repeated top reservoir. It is clear that the seismic response of the model with time-processing derived velocities (figure 2.3a) has failed to give a complete and correct image from the crestal part of the faulted anticline whereas in the seismic response from the velocity model controlled and guided by well information the folded (reflector 1, figure 2.3b) and faulted part of the top reservoir (reflector 2, figure 2.3b) are clear.

The horizons of interest in structure 'B', Masjede-e-Soleyman is the steeply dipping thrust plane and the roll over of younger strata under the thrust plane when it flattens towards southeast (Figure 2.1). The imaged thrust, places the older rock units over the younger units. Figure 2.4a and b show the results of NIP ray tracing for both processing derived velocity and well derived velocity models. The arrow in both figures shows the thrust plane reflector and it is possible to follow it in both velocity models. The geometry of a wedge shaped generated by the thrust plane reflector on top and another reflector immediately below that (to the left of the arrow in figures 2.4a and b) represents the subthrust play originally proposed by Mapstone, (1978) with less confidence.

Therefore the modelling results confirm the velocity used in the processing of the structure 'B' to a great extent, while the velocities applied in the processing of structure 'A' are wrong.

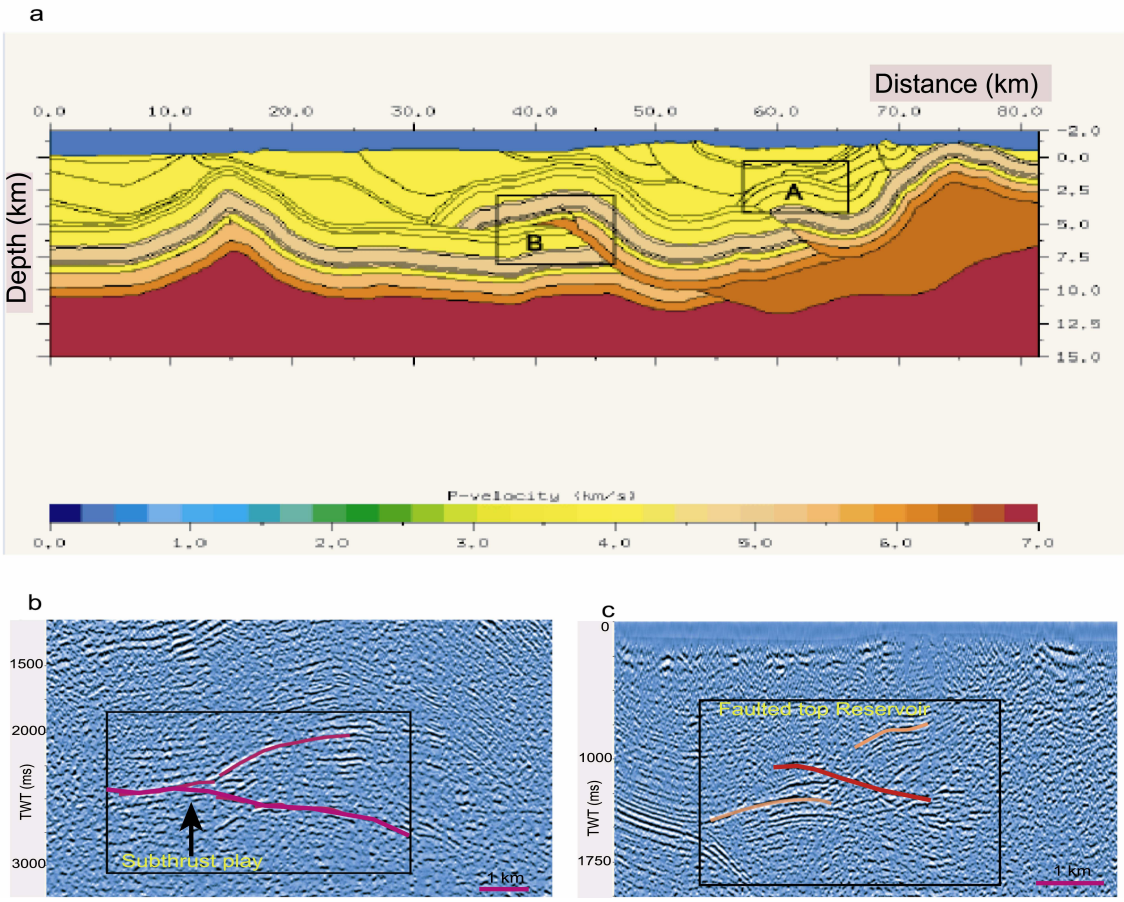


*Figure 2.1 a) Geometry of the macro-model (81km by 17km) together with P-wave velocity variation. The velocity model is derived from time processing velocity data. The blue zone above the surface is air velocity. Locations A and B are the detailed studied areas. (In all figures of chapter 2 the right side is northeast and the left side is southwest). b) 2D poststack time migrated seismic section showing structure 'B', the arrow shows the location of a possible subthrust play. The picked horizon right above the arrow is believed to be a thrust plane reflection. c) 2D poststack time Migrated seismic section of structure 'A'. The picked event is the repeated top reservoir as a result of faulting.*

The velocity model derived from wells used at the next step for NIP ray tracing and the results for structure 'A' represents top of the structure clearly (figure 2.3b).

The second ray-tracing mode applied is image ray tracing. Image ray tracing is an approximation of migrated data that can be called simulated time migration (Hubral, 1977). The ray path that represents the minimum on the time reflection surface emerges perpendicular to the recording surface. Image Ray tracing has been applied both for structures `A' and `B', with two different velocity models derived from processing data and well data.

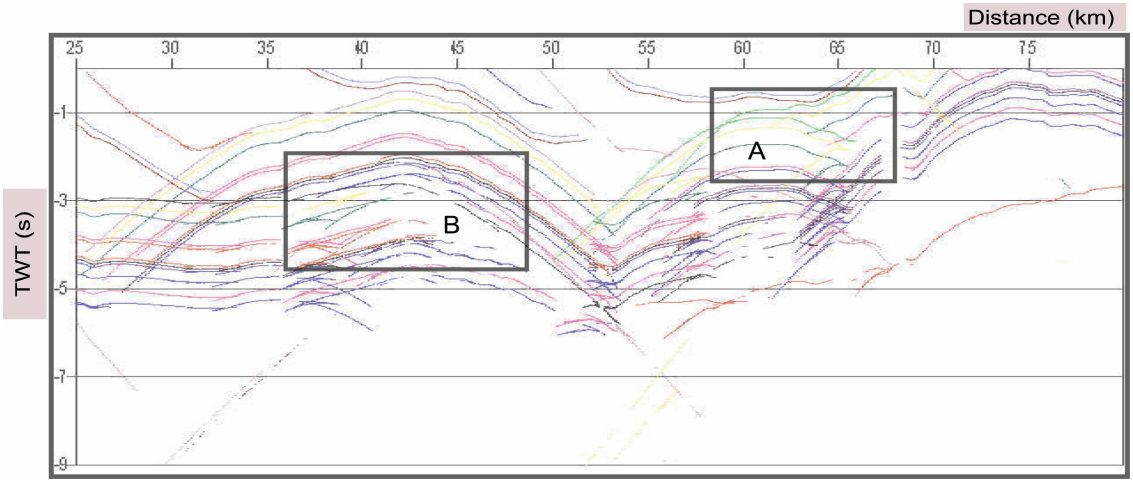


*Figure 2.2 Normal Incidence ray Tracing results (TWT section) of the macro model from the 25th to the 80th km. The location of structures A and B is marked by rectangles.*

The travel times of Image Ray tracing were then convolved with a Ricker 35 Hz zero-phase wavelet. Figure 2.5a and b shows the results of image ray tracing for structure 'A'. It is clear that the crestal part of the structure 'A' shows a gap in the processing-derived velocity model (figure 2.5a), while in the well-derived velocity model (figure 2.5b), there is no gap and the structure top is imaged clearly. The two different velocity models give more or less the same results for structure 'B'. Imaging the steeply dipping (towards the northeast) part of the thrust plane (ramp

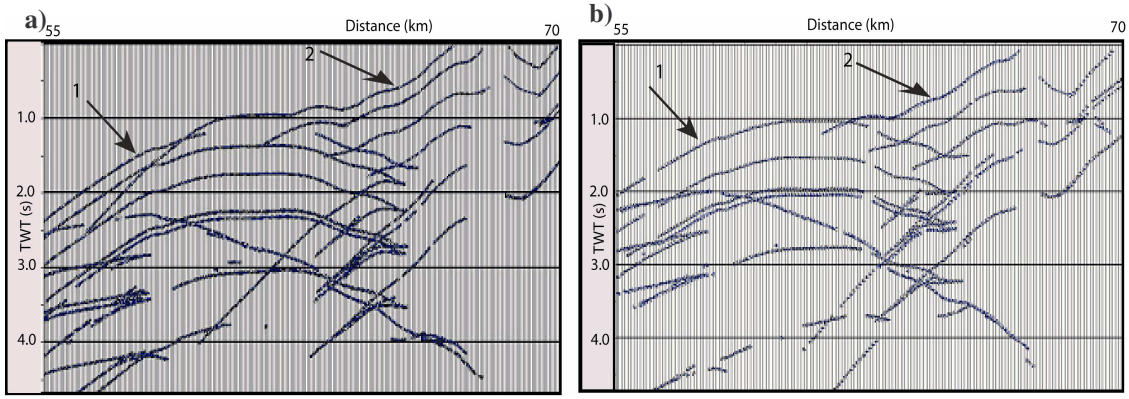


*Figure 2.3 a) Normal Incidence Ray Tracing of structure 'A' with processing derived velocity model b) Normal Incidence Ray Tracing of structure 'A' with well derived velocity model, Reflectors 1 and 2 are folded and faulted top reservoir respectively.*

part) is particularly important. In order to improve the image and to get more consistent data, different migration apertures (from 2 to 10 km) have been tested during image ray tracing of structure 'B'. The result shows that the aperture used in the processing of the real data (less than 3km) was not sufficient to image the steep northeast flank of the structure properly.

This is one of the reasons for poor quality image in the real migrated seismic data (Figure 2.1b). Figure 2.6a shows the results of image ray tracing with 4 km migration aperture and figure 2.6b

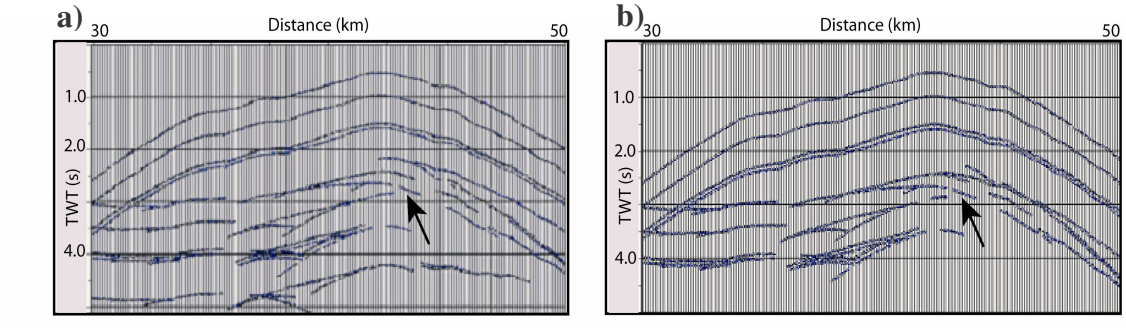


*Figure 2.4 a) Normal Incidence Ray Tracing of structure 'B' with processing derived velocity model b) Normal Incidence Ray Tracing of structure 'B' with well derived velocity model, The arrow shows the thrust plane reflector. The truncation of the reflector below the thrust plane forming wedge shape geometry interpreted as a subthrust play.*

shows the results of image ray tracing with 8 km migration aperture. As can be seen from the results by increasing the migration aperture the steeply dipping hanging wall block become clearer.

The final ray-tracing mode applied is shot gather offset modelling. This resembles the real acquisition. Shot gathers, or common shot gathers are traces recorded at a series of receivers propagating from a single source. This is the way data are collected and its results could be useful in evaluation and design of seismic surveys. One of the important applications of asymptotic methods or ray-tracing methods is the modelling and identification of specific events on seismic records (Carcione, et al., 2002). An off-end source-receiver array has been used to acquire the real seismic dataset. The same source-receiver array has been selected for modelling. From the 35$^{th}$ to

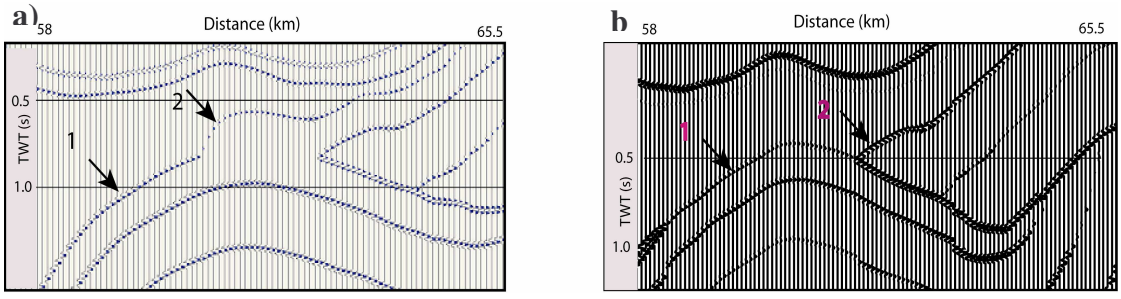


*Figure 2.5 a) Image ray Tracing of structure 'A' with processing derived velocity model, The folded top reservoir (reflector 1) is not continuous, and b) Image ray Tracing of structure 'A' with well derived velocity model, The folded top reservoir (reflector 1) is continuous.*

the 75$^{th}$ km (Figure 2.1a), a series of shots have been generated with 200 m near offset, 144 channels, and 50 meters trace spacing. Layers with opposite dip-direction cause events to be recorded in two opposite dip-direction (up-dip events). For example events representing the folded (reflector 1 figures 2.4 and 2.5) and faulted (reflector 2 in figures 2.4 and 2.5) top reservoir

in structure 'A' have been recorded in completely opposite direction. The faulted leg which is shallower have been recorded much earlier in the shots around x=49km. This observation increases the role of offset in recoding the important events from the faulted anticlines with complex overburden. The off-end source-receiver array provides larger offset than split-spread array. These complex events cause severe problems for conventional (NMO/DMO/stacking/Migration) seismic data analysis (Yan et al., 2001).

Due to velocity and structural complexity, rays are bent and there are non-hyperbolic arrival times (Farm, et al., 1993). The shot gather modelling results show that strong lateral velocity variation in the overburden cause poor illumination at deeper target intervals. Further to the northeast of the section (figure 2.1a) where the high velocity carbonate units exposed at the surface high velocity behaviour of the near surface rocks cause complexity. These facts (strong lateral velocity

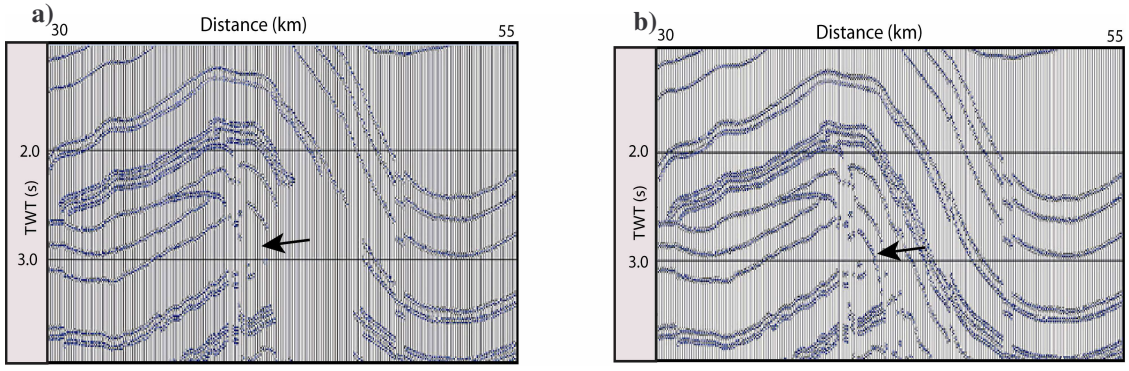


*Figure 2.6 Image ray tracing of structure 'B' with well-derived velocity model, a) migration aperture 4km, b) migration aperture 8km. Increasing the aperture improves the continuity of events in the steep flanks of the faulted anticline.*

variation, steep dips folded and faulted beds, high velocity rock units near surface) clearly show that poststack imaging methods will not give a correct image of the subsurface. The ray coverage in steeply faulted flanks of structures and in places with thick overburden (with strong lateral velocity variation) is not enough so other seismic modelling methods such as finite difference methods should be tested.

In mountainous areas such as the Iranian Zagros FTB, that have structural complexities at target level and heterogeneities in the overburden, seismic forward modelling is an important method to help in all steps of seismic study including acquisition, processing and interpretation. Since this is the first time seismic forward modelling has been applied to the fault related folds in the Iranian Zagros FTB, the results show the necessity of modelling itself for the area of study, as well as the need to plan more detailed modelling studies. Structures are complex and velocity does not have a simple gradient, but is changing laterally and there is also some velocity inversion, so special

processing procedures, such as prestack Depth Migration, are becoming more important, and for such kinds of imaging methods modelling is essential.

# 3 Pre processing for prestack depth imaging

## 3.1 Conventional time processing

Prestack depth imaging is a more theoretically accurate technique than prestack time migration in areas of significant velocity variations. When correctly applied, prestack depth migration should improve imaging and the alignment of events in depth. Much effort is needed to produce results and the quality of the output does not consistently meet expectations. The theoretical advantages of depth migration over conventional time processing have been known for quite some time (Larner, et al., 1981, Schultz, et al., 1980). Pre-processing steps are crucial to reduce seismic depth migration to a depth-imaging problem. In order to achieve this, critical parts of the conventional pre-processing flow need to be reworked and specifically tuned to depth imaging constraints (Schmid, et al., 1996).

The 3D dataset acquired over Karanj and Parsi oil fields in the mountainous part of the Iranian Zagros FTB was significantly affected by the surface geology. In some areas, high levels of coherent and random noise contaminated data. This may have been due to the difficulty of using deep shot holes and also poor geophone coupling. In fold and thrust belts with strong topographic variation the main pre processing steps are:

1-Exact handling of topography;
2-noise attenuation including source noise,
3-amplitude processing.

Processing tests need to be run for choosing optimized parameters at each of the above steps. A brief summary of the pre-processing jobs that have been applied on the data is as follows (CGG Final processing report):

- Reading from CGG format to SDS (Seismic Data Server);
- Trace geometry updating control;
- Spherical divergence correction. Each sample is multiplied by T x V2 (T is the two-way time; V is an average velocity function);
- Instrument compensation;
- Primary static application to floating datum plane (FDP), Computation from the 3D near-surface model derived from upholes, Correction velocity: 3000 m/s Datum elevation 1300 m;
- 3D FK conical filter (FKx-Ky) in Cross spread domain, - velocity cut-off: 2600 m/s – attenuation: 24 dB;

- Additional gain versus time (3 dB per second);
- Gain versus offset correction;
- Automatic editing of noisy traces, Statistical editing based on average amplitude comparison;
- 3D surface consistent amplitude correction (source and receiver) computed in window 500 – 2000 ms;
- 3D surface consistent spiking deconvolution (zero phase output), multi-channel phase deconvolution (leading to a zero phase output), multi-channel amplitude deconvolution performed in two windows: 400 – 1800 ms, 1200 – 3000 ms, operator length: 200ms, white noise 5 %, spectral replacement of the low frequency part (6 Hz, 36 dB per Oct.).

This 3D dataset is the first three-dimensional seismic data acquisition in the Zagros Mountains. This is a region of great topographic variation and the elevation in the survey area varies between 200m up to more than 800m above mean sea level. Figure 3.1 shows the elevation map for the floating datum (a smooth version of the real topography) of the survey area. Proper surface referencing is necessary when processing of fold and thrust belt seismic data. The near surface is complex and can vary rapidly.

Corrections are applied to seismic data to compensate for the effects of variations in elevation, weathering thickness, weathering velocity, or reference to a datum. The main goal is to determine the reflection arrival times which would have been observed if all measurements had been made on a plane with no weathering or low velocity material present (Cox, 1999). To solve the problem of static corrections, the GLI3D (Generalized linear inversion) refraction method from Hampson Russel, based on first break inversion, was tested and compared with field static and elevation static. Figure 3.2 shows the field static map for the survey. The average visible refractor velocity is 3300 m/s on the first breaks retrieved from the 3D seismic data. The field statics provided by the acquisition contractor BGP are supposed to include vertical time for shot points and interpretation of the low velocity layer (LVL) survey (up-hole shots and refraction shots). Difference between the field statics and the brute elevation statics was computed. The brute elevation static has been calculated with the following equation:

$$Ts = \frac{Zr - Z_d}{V_R}$$

where $Z_r$ is the elevation of receivers and sources, $Z_d$ is the final datum elevation, 1300 m above mean sea level in this project, and $V_R$ is replacement velocity, 3000m/s. The average difference is –5 ms for both receivers and sources. A first break based method has been applied (generalized linear inversion). The results are worse than the field static correction method. Cox, (1999) has

also recommended uphole-based static corrections as first priority. Actually due to poor quality records in some parts methods based on first break picking are more subject to error. The output at this stage (after the 11$^{th}$ step explained above) has been the input for prestack depth imaging.

## 3.2 Additional Noise suppression

Noise in seismology can usually be regarded as a failure of analysis rather than as something polluting the data (Claerbout, 1985). Pre-processing for prestack depth migration as in time processing can have a dramatic effect on the final results. Since the data will be analyzed before stack, it is very important to have the data as clean and noise free as possible. There were many spikes in the data that will make the migration results noisy. A main reason that prestack time migration techniques produce good signal quality is that they have great leverage in the choice of velocities used to produce a good stack. They have this leverage because the positioning of events in time migration is less sensitive to the errors in velocity than depth migration. Furthermore, in some implementations of prestack time migration, separate velocities are used for stacking from those used for imaging. This separation gives prestack time migration greater leverage to produce a good stack. Therefore for prestack depth imaging more noise suppression should be done on input seismic data. In order to see the effect of spikes in the image quality a test prestack depth migration has been run. Figure 3.3 shows an inline example from this test migration. The image is dominated by migration-related noise and the spikes have also generated specific noises that have been marked in the figure.

For depth imaging purposes I have run the following job to reduce the noise contents. The job detail is as follows:

- Band pass frequency filter (5,15,60,75 Hz for T0-T1000 and 5,15,40,60Hz for T2500-T6000);
- Specific frequency noise removal. This was done by mono-frequency attenuation (noise estimated adaptively and then the estimated noise subtracted from the traces). The selected frequencies are: 22, 33, 44, 50, 55 and 61.

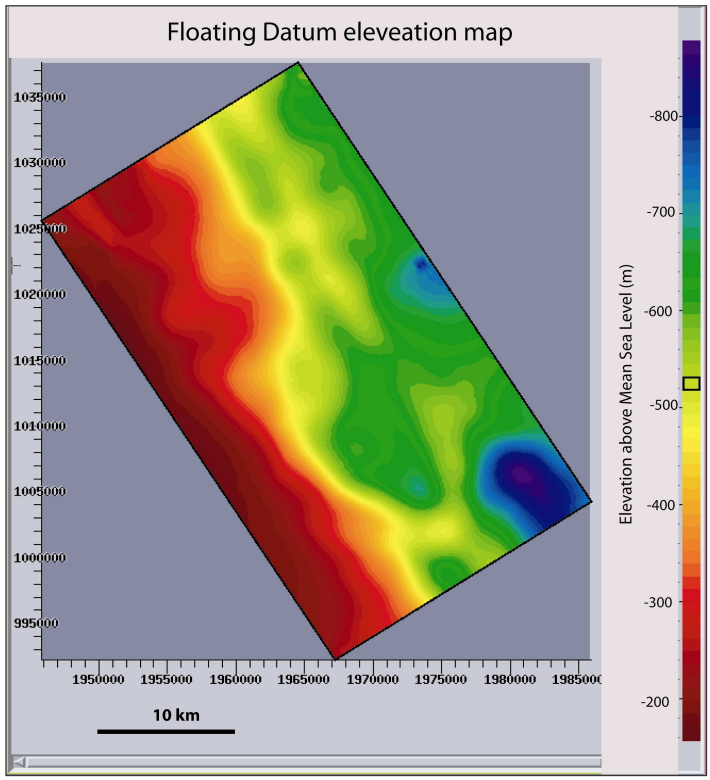


*Figure 3.1 Floating datum elevation map of Parsi and Karanj 3D survey. The elevation ranges from 200 up to more than 800m above seal level.*

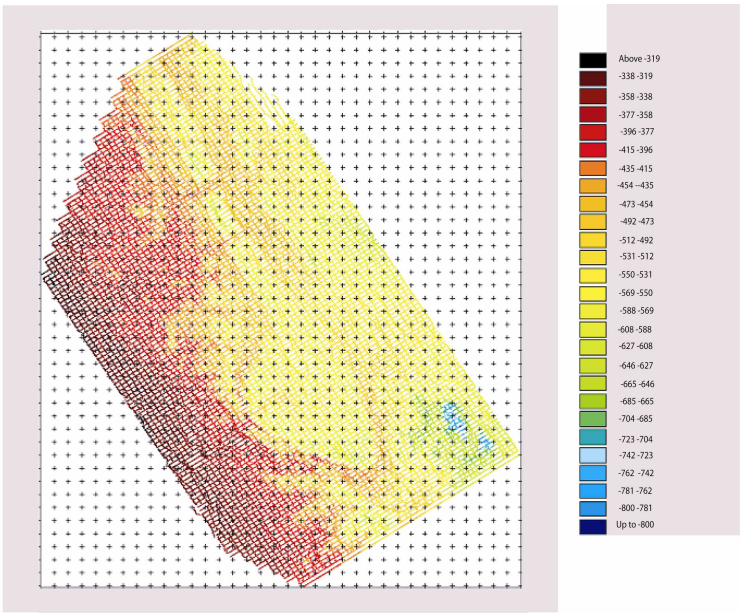


*Figure 3.2 Field static map (CGG, 2003)*

- Inner and outer mute application allows attenuating effect of remaining multiples and also avoids migration of noises of far offsets. The inner mute values were (X, T; 0, 800; 400, 1300; 450, 5000). The outer mute values were (X, T; 0, 0; 3200, 700).
- In order to improve the resolution of the upper part of the data a time variant Butterworth filter was applied to attenuate high frequency content in the lower part of the time gathers.

Trace scaling with 50 percent overlapping. Figure 3.4a and 3.4b show a time gather before and after running the job explained above. Data are more uniform and the noise content has been reduced to a considerable degree.

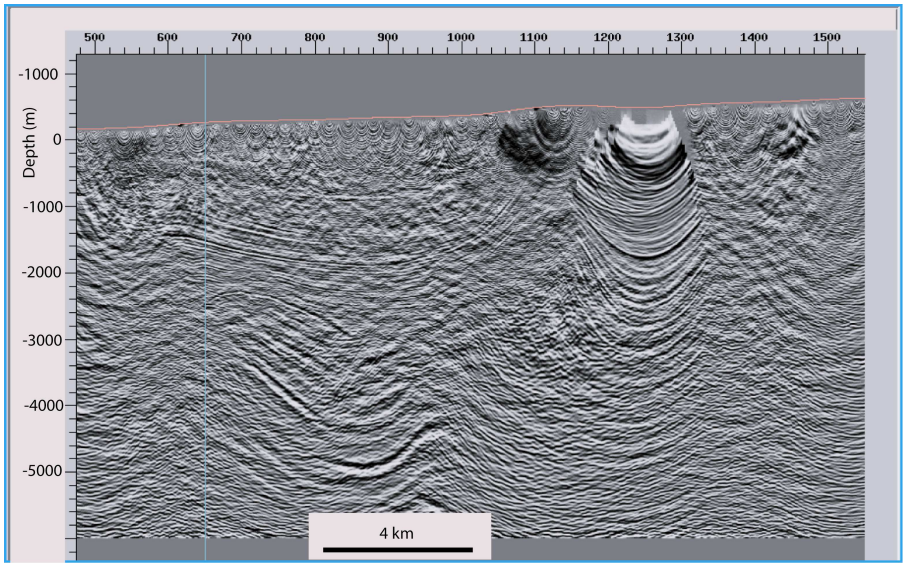


*Figure 3.3 the results of a test PSDM with the time gathers before eliminating the remaining noise of the input data.*

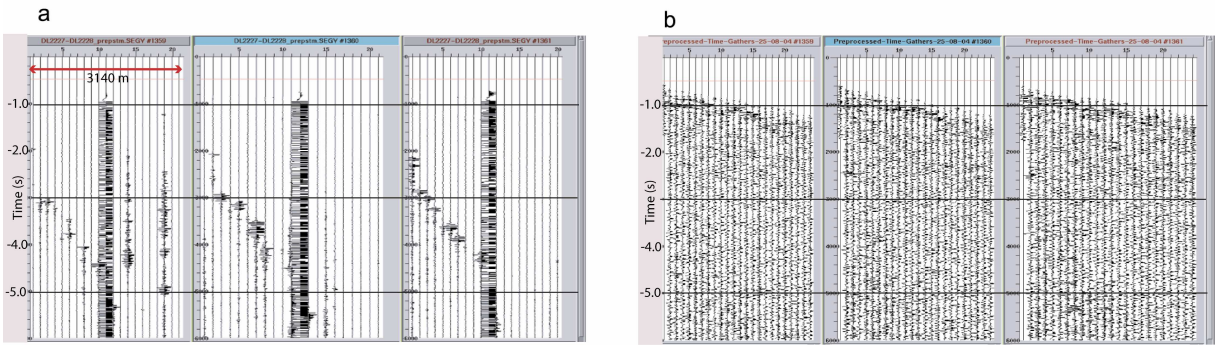


*Figure 3.4 a) prestack time gathers before running pre processing filtering job, b) the same prestack time gathers after running the pre processing filtering job.*

# 4 Migration velocity analysis using hybrid tomographic approaches

## 4.1 Introduction

In complex structures lateral velocity variations cause a nonhyperbolic component to be added to the CMP gathers therefore, accurate knowledge of seismic interval velocities is essential for imaging. In order to find the correct laterally varying velocity field, analysis in the prestack domain can resolve the nonhyperbolic moveout component.

The State-of-the-art and widely used method for velocity estimation is global tomographic methods that give structurally consistent results and is (Stork and Clayton, 1991, Stork, 1992, Clapp, et al., 2004, Van Trier, 1990, Etgen, 1990). Prestack migration contributes far more than its ability to provide imaging results and it has been used to measure the quality of the estimated velocity (e.g. Al-Yahya, 1989, Faye and Jeannot, 1986, Van Trier, 1990, Woodward and Albertin, 2004, Soazig, et al., 2004). Velocity determination by prestack imaging is an interactive method and analyzes CRP gathers and constant offset sections.

The main concept is that when the applied velocity is correct the migrated data from different domains such as different shots, different angles and different offsets will give an identical subsurface image. This is because they represent the same subsurface area. If the applied velocity is not correct then the images from different domains are not properly aligned. The difference can be used to correct the velocity. Tomography back projects these residual moveout on gathers to modify the input velocity model. An important part of any method is how effective the consistency of the results can be measured. Tomography is also useful because it updates the velocity globally. For depth imaging an estimate of the interval velocity at every point in the subsurface is needed, not only at every imaging point. In so called single station methods velocity analysis carried out at one CRP location using a small number of gathers around the location and it is assumed that the velocity changes are independent of the analysis in other points, i.e. that they are structure independent (Yilmaz, 2001).

Irrespective of the method used to estimate velocity, there is unfortunately usually more than one model, which satisfies the observed data. In other words the velocity determination problem is non-unique or an ill-posed inverse problem (Sexton and Lemaistre, 2004, Tritel and Lines, 2001). Non-uniqueness of the inversion methods is due to such factors as:

limited seismic bandwidth, data acquisition limitations, e.g. energy penetration problems at deeper levels, and noise content of data. The reflection method itself is the main source of non-uniqueness insofar as sources and receivers in surface seismic measurements do not surround the object we are attempting to image. The use of a simplified theory of wave propagation (e.g. not accounting for factors such as scattering, dispersion due to attenuation, high frequency assumptions etc.) also gives rise to non-uniqueness.

The general solution is to impose some sort of a priori information or additional constraints to control the results of velocity determination methods and force convergence to the correct velocity field. There are at least two ways of imposing such a priori information on the inverse problem solution. In the first approach more emphasis is placed on modifying the back projection formulation with the a priori information. To control the accuracy of the results and produce the best model Stork and Layton, (1992) use the geologic constraints in the form of a variety of simple filters. Rowbotham, et al., (1997) incorporate the non-seismic information into the null-space model singular vectors. The second approach is to control the results by some kind of a priori information. One of the most common and also practical ways to constrain the velocity determination process is through seismic interpretation. Velocity model building is far more effective when strongly linked to an interpreted structure (Fagin, 1999). The final goal of seismic imaging is to give an image of the subsurface and if the structural interpretation is involved during the process it will definitely provide better and more consistent results. An interpretational velocity analysis approach in seismic exploration ensures the development of accurate results. The general belief in the industry is that results of velocity analysis are geologically plausible when a sound interpretation effort is put to in the data analysis (Yilmaz, 2001). This means that the initial velocity model and the resultant seismic image must no longer be considered as the final output of seismic data processing but rather as intermediate steps in an iterative sequence, in which geological interpretation of the seismic image helps in obtaining a better velocity model.

## 4.2 The integrated method

In the present study an integrated velocity estimation method has been defined. The method includes depth tomography of prestack migrated gathers. The velocity analysis procedure is constrained by using different a priori information at different stages of the velocity estimation procedure The main a priori information consists of well logs, vertical seismic profiling data, knowledge of structural style in the studied area, and detailed seismic interpretation. The wells are used to control the vertical behaviour of velocity from the beginning of model building. The proposed procedure for migration velocity analysis is shown in figure 4.1.

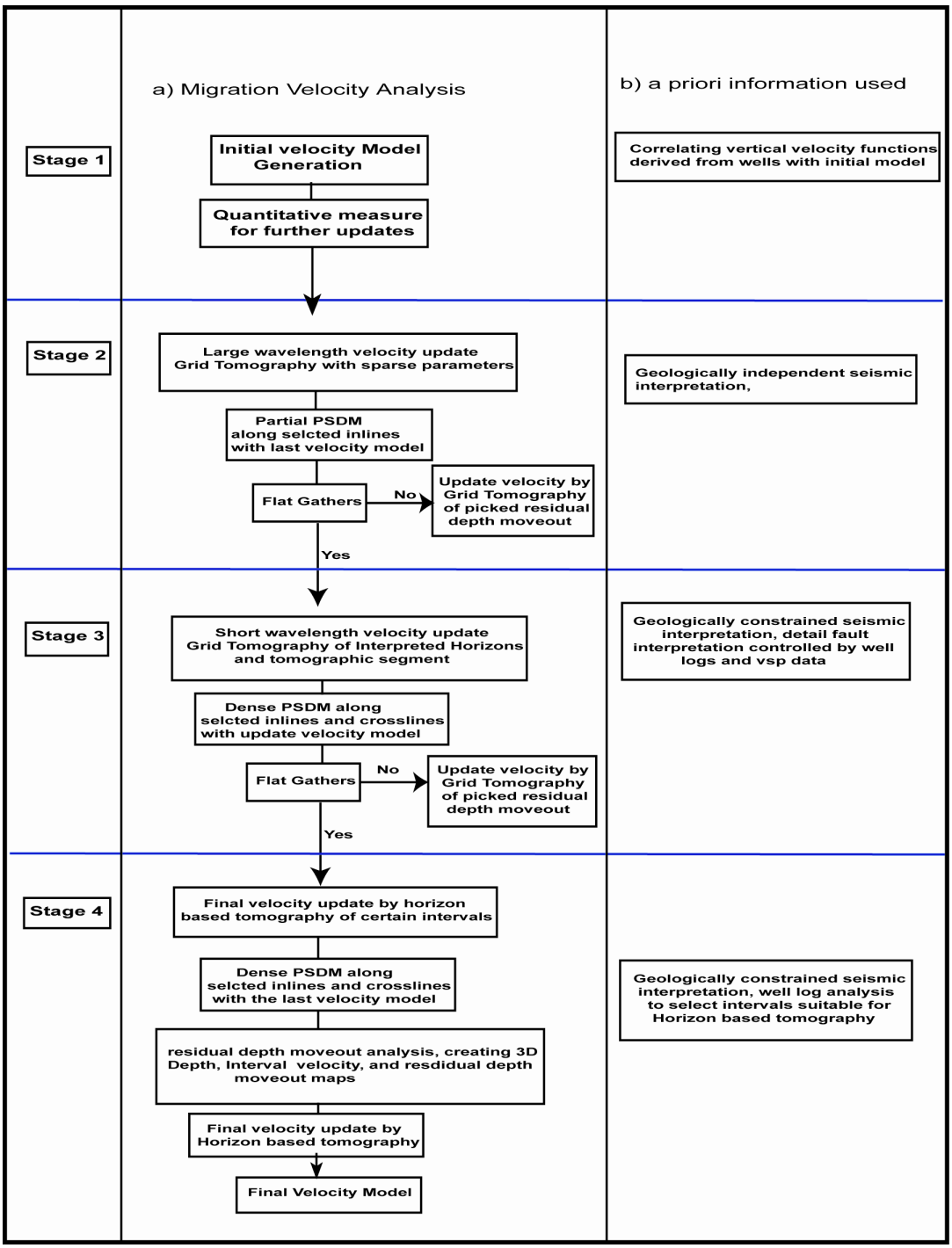


*Figure 4.1 The defined flow for migration velocity analysis in complex fault-related folded areas. The left column is the inversion detail including different tomographic methods applied at each stage (a) and the right column (b) is the a priori information used to constrain the inversion at each stage. The flow consists of 4 main stages: Initial model generation, regional velocity update, high-resolution velocity update and final model generation.*

### Stage 1 Initial model generation

The common approaches for migration velocity analysis is migrating the data using a velocity model and sort the gathers (common offsets) and then look for any residuals since zero moveout is generally accepted as a measure of optimum velocity. It is recommended to start with a simple initial velocity model. A simple 1D velocity model can be derived from time processing steps. An initial interval velocity model can be built using velocities from pre-stack time migration, i.e. RMS velocities (Yilmaz et al., 2000) or stacking velocities. If the initial model is very different from the correct one it may need several iterations to obtain the final model or it may even not converge to the right answer. Therefore it is important to keep it simple and at the same time make it as close as possible to the correct model. In order to achieve this two following steps are suggested:

1-Check the resultant velocity cube for any possible short wavelength anomaly that may be generated by the Dix conversion process. It is better to select coarser depth intervals during initial model generation and change to finer depth intervals later in the velocity estimation procedure.

2-In order to obtain an estimate of the difference between the initial velocity model and the final correct one, vertical interval velocity functions derived from well data (wells with reliable logs) can be compared with vertical interval velocity functions extracted from the initial velocity model. These two different velocity functions from the same point in the data will provide a good quantitative measure of the difference between the initial velocity model from a correct model at well locations. This step should be done with caution since there are factors such as anisotropy that control the velocity function and the initial model has been built assuring isotropy.

After this comparison the amount of updating needed for each interval becomes clearer. Therefore more effort can be put on intervals that require more updating. In the complex faulted folds that are the subject of this study it worth mentioning that there should be a minimum number of wells and any evaluation based on, for example, one well only will be subject to errors. If a well is located in a hanging wall block of a faulted-fold we cannot apply the exact velocity behaviour for the footwall block of that particular fold. So the application of well information should be in the context of the structural style of a complex geometry.

### Stage 2 Regional velocity update

At this step that has been called regional velocity update or long wavelength velocity update the macro velocity model is obtained. Partial Kirchhoff prestack depth migration runs along selected inlines (coarse intervals for regional updating purposes) with the initial velocity field. The representation of the subsurface is important for type of tomographic velocity update to be used.

Two different tomographic methods are in common use now. Grid-Based or cell-based tomography and layer-based tomography. In the grid-based approach the subsurface is represented by a 3D velocity grid that has a velocity value each node and the interval velocity values of these nodes are updated in the tomographic iterations. The important advantage of grid tomography (Koren, et al., 1999, Woodward and Albertin, 2004) is in areas of such complex geology that a detailed structural framework cannot be achieved in early iterations of the velocity updating from the existing depth images. In these cases, grid based tomography can be applied without the complete interpretation of reflecting events in the whole area. So, at this stage grid based tomography is applied.

The interpretation is just used to pick some strong amplitude or coherent events from the migrated stack sections, not to make a complete depth model. Events that are not part of the depth model can serve as input to tomography. The residual depth moveout of the picked events is derived using semblance analysis. Semblance is calculated along the picked horizons using a residual moveout analysis technique and the 'residual moveout' has been picked where the semblance value is maximal. The residual depth moveout for the picked events is transformed to time moveout and using this better velocity can be found. The residual moveout is a measure of the non-flatness of the gathers after migration. The grid tomographic principle attributes an error in time to an error in velocity. The tomographic approach attributes the value of the time moveout to the accumulation of errors within that depth interval.

At this stage, since the velocity volume is being updated regionally, it is not necessary to select dense grid spacing for tomography. It is important to know that at this stage the velocity update is mainly data driven. The resultant velocity after each update will be used to run another partial PSDM and the only way to control the results is to verify the image quality and general convergence towards the structural pattern of the complex faulted-folds. The residual velocity volume, which is the difference between two successive velocity updates, also gives an idea of convergence. The sequence of partial PSDM, seismic interpretation of coherent events, residual depth moveout analysis, and grid tomography is repeated until the regional structural framework is achieved.

### Stage 3 High resolution velocity estimation

The updated velocity model can now be used for the next PSDM. Since the resultant velocity volume from the previous stage has improved the coherency of the seismic image, more horizons can be picked and some of them can also be picked with larger coverage than in the previous stage. Since the generation of an accurate depth model needs an accurate interpretation that includes the exact geometry of structures for obtaining high-resolution velocity update, I suggest

running grid tomography of both fully interpreted and partially interpreted horizons rather than using horizon based tomography. A priori information at this stage is: 1-From wells: vertical velocity functions, marker depths, and 2-Structural seismic interpretation in detail that includes thickness maps of interpreted horizons, detailed interpretation of internal structural elements in the overburden, and mapping the main thrust faults and related folds. The accuracy of the depth model generated at this stage is checked by all available well information and also knowledge of the structural style. The grid tomography of the depth migrated gathers modifies the velocity field with greater resolution at this stage. The resultant velocity field represents the main and detailed structural elements of the faulted folds.

### Stage 4 Final velocity update

This is a stage that requires prior study of the interval velocity character of the geological formations using well logs. If there is not enough well control the third step could be the last one particularly when 3D seismic surveys are run for exploration purposes. There are some rock units, such as carbonates, that have little velocity variation vertically so the vertical velocity variation is more or less depth-independent. There are other rock units such as clastic rocks in which vertical velocity variation is more pronounced. The velocity variation in carbonates is more dependent on the environment of deposition (Anselmetti and Eberli, 1993, 2001). Carbonates are common in many geologic sections of the world's hydrocarbon fields e.g. western Canada and the Middle East. In such cases interval velocity varies between the interfaces more than within layers. In these cases the abrupt changes of velocity at the interfaces cause ray path bending and therefore must be explicitly dealt with. This type of velocity variation (along the interfaces) is ideal for horizon-based tomography.

Horizon based tomography is carried out in 3 steps: I) Performing residual depth moveout analysis, II) picking residual depth moveout and creating residual moveout models and III) performing tomography to update the velocity and interface depth globally. The horizon based tomographic (Koren, et al., 1999) principle attributes an error in time at one location to an error in velocity and depth (Kosloff et al., 1996, Biondi, 2004). For the selected interfaces of horizon-based tomography the cross-plot of interval velocity derived from wells is a good measure for modifying the interval velocity map of the particular horizons. The velocity model generated at the end of this stage is the final one. In complex fault-related folds making a depth model is difficult and this is why I suggest running the horizon-based tomography at the last stage of velocity updating.

## 4.3 Field Example: Parsi and Karanj 3D, Zagros Mountains

The proposed procedure for migration velocity analysis explained above has been applied to Parsi and Karanj 3D dataset from the Zagros FTB (figure 1.7). The main acquisition problem is poor illumination under plastic rock units. The energy of near vertical events below these thick sequences is not enough to reconstruct the correct image. A wide-angle reflection method has been tested in the Zagros FTB that showed a slight improvement. The global offset technique that has applied in the southern Apennine region southern Italy which consists of fixed geophone array every 90m with a maximum offset of 18km (Dell'Aversana, et al., 2003) can be tested in the Zagros FTB to investigate first the possibility of obtaining better illumination under the thick plastic sequences and second to obtain a better understanding of complex fault-related geometries in the deeper levels.

Figure 4.2 shows a general interval velocity function of the studied area that is applicable for most of the structures located in the Dezful embayment. Units 1,2, and 3 are the overburden interval. Unit 1 is the shallowest part and includes Bakhtiari, Aghajari, and Mishan formations. The velocity variation in this interval is more or less depth dependent. Units 2 and 3 are representing Gachsaran formation. This is the most difficult interval (units 2 and 3) in the overburden in terms of velocity analysis. The higher velocity intervals in unit 3 are part of the Gachsaran formation that is mainly composed of salt. Units 4, 7 and 9 are the main carbonate layers (reservoir) in the Dezful embayment. Units 5 and 6 and 8 are the intervals with lower velocities surrounded by high velocity carbonates of units 4, 7 and 9.

### Stage 1 Initial model

The initial model for interval Migration Velocity Analysis (MVA) has been generated from both stacking velocity and PSTM velocities (RMS velocities). Using RMS velocities of PSTM has been suggested (e.g. Yilmaz et al., 2001) because they are generated in migrated domain and take the advantage of the focusing capabilities of migration (Biondi, 2004). Figure 4.3a and figure 4.4a are two examples of initial models of two different lines generated from stacking velocity and RMS velocity respectively. Up to the end of regional velocity update I have not observed any difference between the results achieved by different initial velocity models.

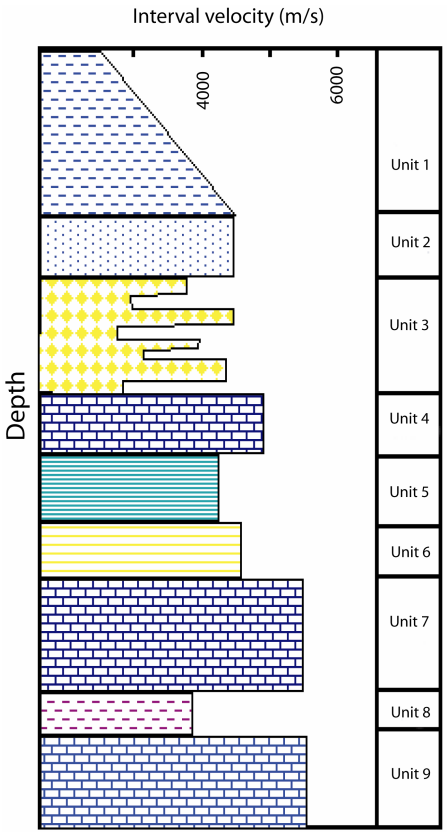


*Figure 4.2 Generalized vertical interval velocity function of the Dezful embayment. Units 1,2 and 3 form the overburden and unit 3 has several internal complexities. Units 4, 7 and 9 are the main carbonate layers in the area. Depth is not in scale.*

## Stage 2 Regional velocity update

Figure 4.3b is an example of the result of the second stage of velocity updating (long wavelength velocity updating). The updated velocity model at this stage reflects the regional structural framework of the area. The red interval marked in figure 4.3b is the high velocity carbonate layer that is separated to two different blocks. These two blocks represents Parsi structure to the right and Karanj structure to the left. The line drawn in the shallow part of the section shows how

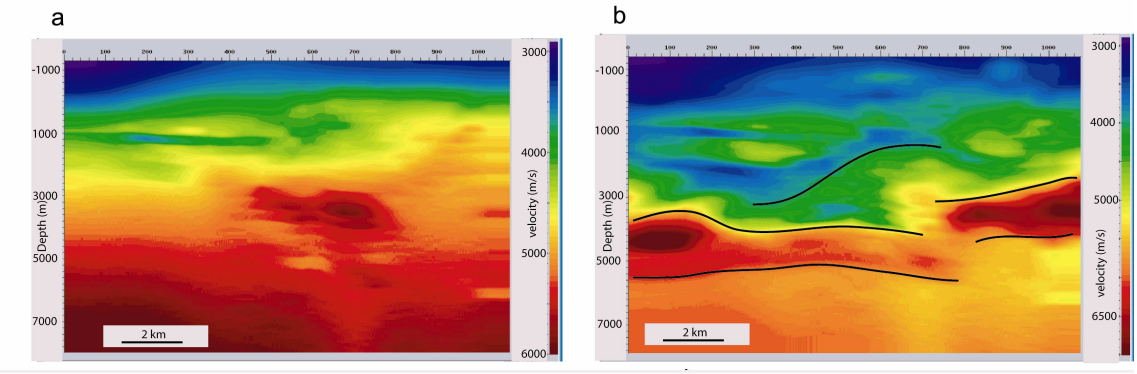


*Figure 4.3 a) Original velocity model derived from stacking velocity through Dix conversion, b) The same inline after the second stage of velocity update. Regional structural framework is revealed. The red interval is the high velocity carbonate. The line in the shallow part separates the low velocity interval (blue above the line) from the high velocity (salt beds) units below.*

velocity reflects the structure in the overburden interval and also clearly shows the different

structural style with the carbonate unit below. The blue zone above the drawn line in the overburden is representing the low velocity layers in the Gachsaran formation (units between the salt beds). Figure 4.4a and b shows another example of regional velocity update along crossline. . The low velocity unit 5 is below the red interval of unit 4 (carbonate layer)(figure 4.4b). Unit 4 and the interval below are divided into two parts by thrust faulting. This is represented by velocity update (figure 4.4b). The interpretation used at this stage has not controlled by wells and only the events with good continuity have been picked. The regional velocity structure was achieved after 3 iterations of partial prestack depth migration, geologically independent seismic interpretation, and residual depth moveout analysis and grid tomographic velocity updating.

### Stage 3 Short wavelength velocity update

At this stage interpretation is being checked by well information and the depth model was built. Grid based tomography have been applied again with improved parameters. Figure 4.5a shows an example of the high-resolution velocity function obtained at this stage. Unit 3 is separated from unit 2 above. The background is the PSDM section. Figure 4.5b is another example showing the structural consistency of the velocity field. The velocity model reveals a remarkable level of structural detail. For example the hanging wall and footwall blocks together with the geometry of the thrust plane are easily distinguished in the velocity model Lower velocity units 5 and 6 follow the high velocity carbonate unit 4. The red interval below unit 5 is the high velocity carbonate unit 7. A structural style difference between the overburden (synclines of units 2 and 3 at the right side of the section) and the target interval (Anticlines of units 4,5, and deeper levels) is reflected in the velocity model. The velocity field is structurally consistent and reflects the structural detail as well as lateral velocity variations and velocity inversions. For the third stage the above sequence was repeated totally five times to obtain the high-resolution velocity model.

As stated earlier when the applied velocity for PSDM is correct the migrated data from different domains such as different shots, different angles and different offsets (CRP gathers) will give an identical subsurface image and will be flat. Figure 4.6a shows an example of the CRP gathers using the high-resolution velocity model. The events are flat. Figure 4.6b shows the horizon based residual move out analysis for two horizons.

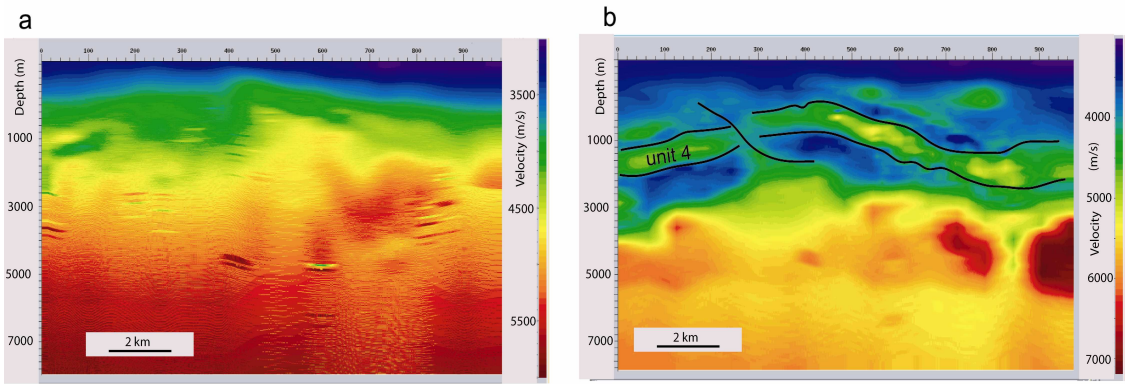


*Figure 4.4 a) Original velocity model derived from RMS velocity along a cross line (Karanj structure). No velocity inversion is included in the model. b) The same cross line after the regional velocity update. The main structural elements are included in the model. The high velocity carbonate unit 4 can be followed along the line. The effect of the thrust fault cutting the units 4 and deeper intervals is also evident in the velocity function.*

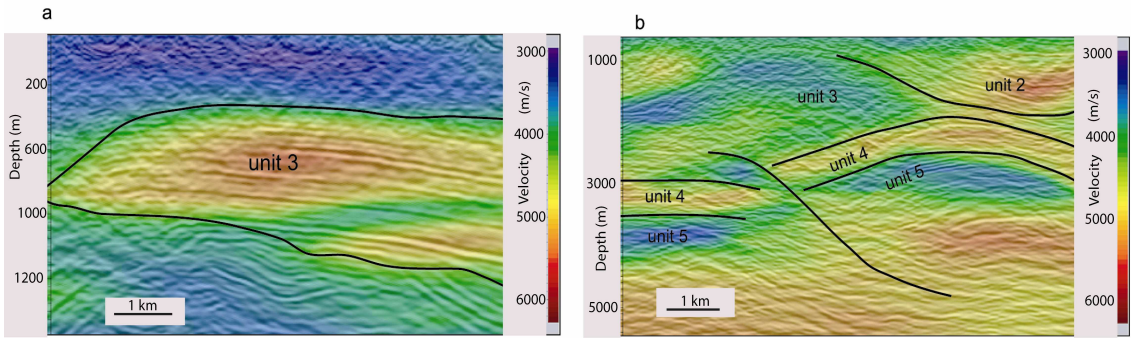


*Figure 4.5 High-resolution velocity model resulted after the third stage of velocity update. The background is the migrated depth image. a) The wedge shape is representing unit 3. The lateral velocity variation of the overburden is included in the velocity model. b) Inline showing the structural detail. Thrust fault and the hanging wall and footwall blocks of units 4 and 5, together with velocity inversion in unit 5 are included in the model. The different folding style of units 2 and 3 (overburden) with respect to units 4 and deeper is reflected in the velocity model.*

## Final velocity update

The detail depth model is built using the horizon picks that is controlled by more than 90 wells. The faults also included in the model as well. Figure 4.7a shows the solid model built for horizon-based tomography purposes. The velocity variation in carbonates (units 4, 7, and 9) is more dependent on the environment of deposition and vertically there is less or almost no depth dependent velocity variation in these units. But there are strong velocity changes in the boundaries of these units with the units above and below. This makes them good for horizon based tomographic velocity update. The last stage of tomographic velocity updating includes horizon based tomographic updating for the intervals explained above. The velocity model is reflecting

the stratigraphic detail as well as structural detail and makes proper focusing possible during migration. Figure 4.7b shows an example of the velocity update with horizon-based tomography. The different velocity units have been differentiated. When there is not enough well information and the subsurface is complex building a complete depth model is difficult so the horizon-based tomography become very unstable.

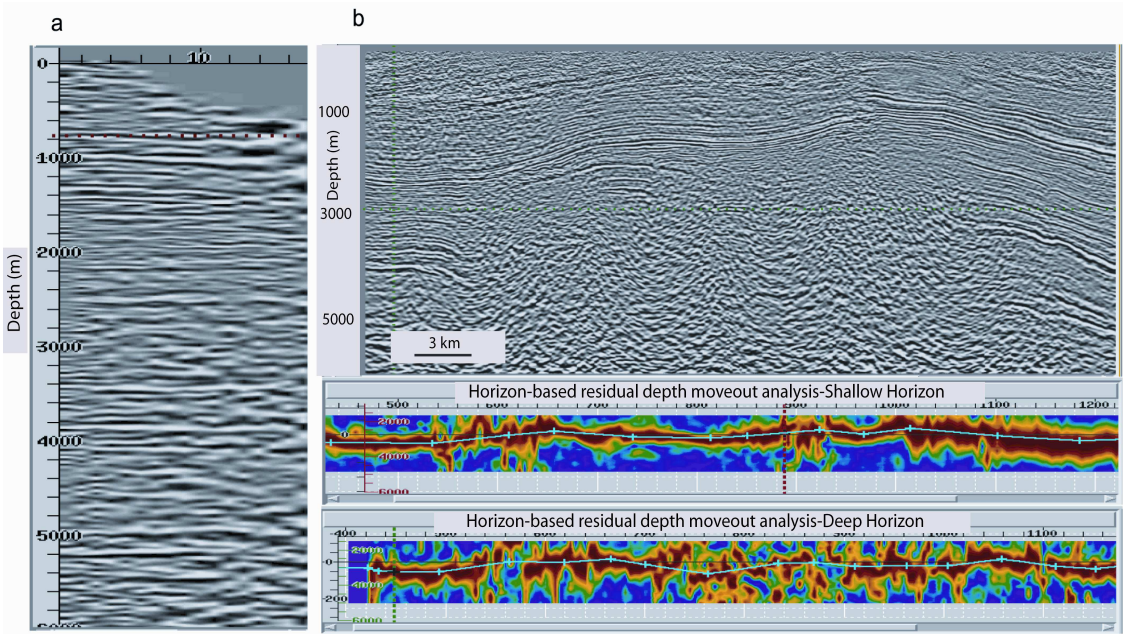


*Figure 4.6 a) A sample Common Image Gather after the third stage of the velocity update. The events are flat and there is more or less no residual depth moveout. b) Horizontal semblances for two horizons, one in the overburden and the other in the target interval after the third stage of the migration velocity analysis. The residual depth moveout has decreased to very small values.*

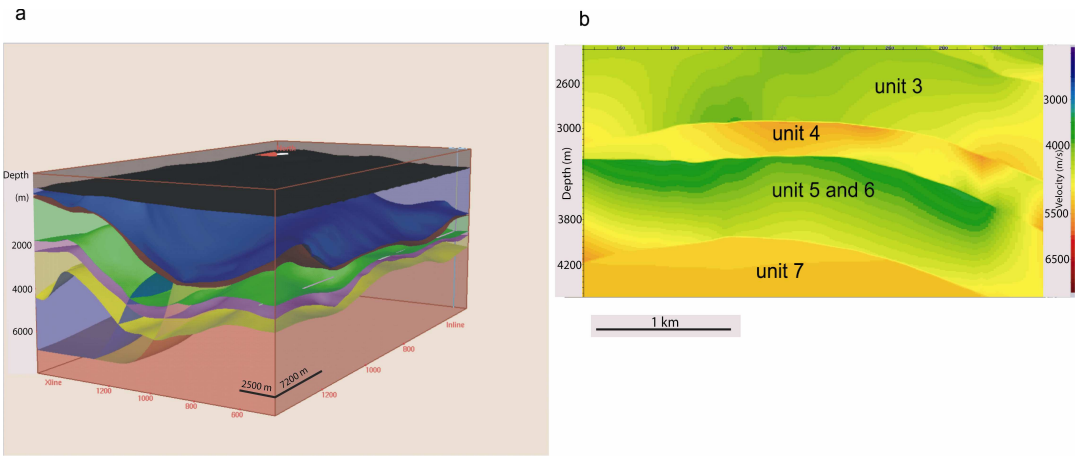


*Figure 4.7 a) The final depth solid model after third stage of velocity update. It includes horizons from units 3, 4, 5, 6, and 7. The faults are also included in the depth model. b) The final velocity model after fourth stage of velocity update. This stage includes horizon-based tomographic velocity updating of certain carbonate intervals. The solid depth model is used in the tomographic velocity update.*

# 5 Single arrival Kirchhoff PSDM of complex faulted folds from Zagros FTB

## 5.1 Prestack depth migration in complex faulted structures

Migration is an important stage in seismic imaging that focuses the seismic recorded data and generates a true structural image from subsurface. It removes the effect of seismic wave propagation (e.g. diffraction from sharp edges) from data, therefore seismic events move towards their correct subsurface positions. In complex fault and fold thrust belts with rough topography, migration is difficult due to lateral velocity changes and also very steep dips. Prestack depth migration is the state of the art solution for seismic imaging in such situations (e.g. Yan, et al., 2001). The geometry of acquisition in the complex geological situations with rough topography is seldom regular so the Kirchhoff prestack depth migration is the method of choice (e.g. Biondi, 2004). Since it is less sensitive to irregular spatial sampling of 3D prestack data. It has also the possibility of target oriented processing and input/output flexibility and computation efficiency (Audebert, et al., 1997). Kirchhoff migration (Schneider, 1978, Docherty, 1991, French, 1975, Audebert, et al., 1997) is based on Green's function theory and an integral solution to the wave equation. The summation surfaces are the basis of the Kirchhoff migration and in terms of physical interpretation they are diffraction surfaces for point scatterers located in the subsurface. In structurally complicated areas, seismic imaging is difficult and needs interpretation to be involved (Gray, 2000).

The effects of different Green functions have been investigated on the Parsi and Karanj 3D data set from the Iranian Zagros FTB. Any correct depth imaging requires a correct interval velocity model. The acquisition parameters have been explained in chapter 1. The pre-processing procedure is important since it can improve the quality of input data for seismic imaging (both velocity analysis and migration). The main goal of pre-processing is to suppress the noise as much as possible while keeping signals untouched. The main steps of pre-processing applied on the input data before seismic depth imaging have been explained in chapter 3.

The sources of complexity in the studied area are common to most mountainous areas of fold belts. First of all, the near surface problems cause data to be distorted. These include the effects of variation in elevation, near-surface low-velocity-layer (weathering) thickness, weathering velocity, and the reference to a datum. Figure 5.1 shows the poor coverage due to topographic variation. Irregular source and receiver points are shown in the figure as well.

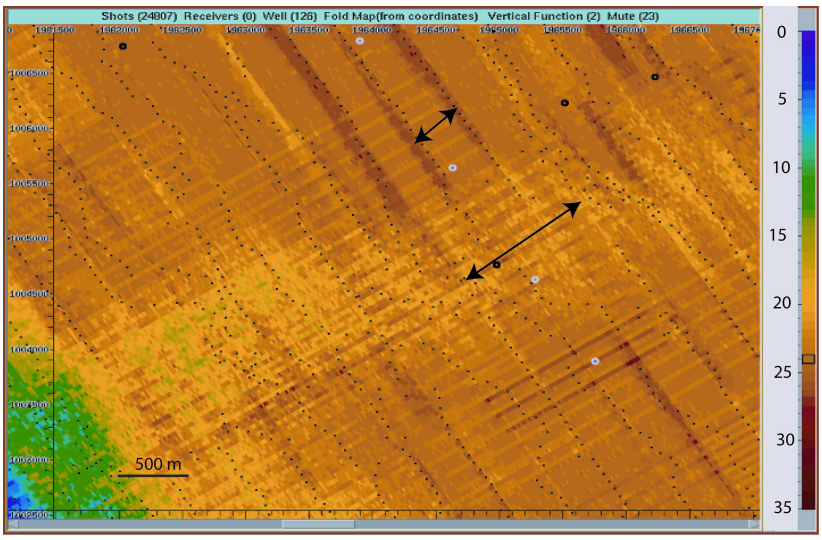


*Figure 5.1 The fold coverage map. The black points are the source points. The planned source line interval is 400m but the source points location changes due to topographic variation. The longer arrow shows location with more than 800 m source line interval.*

The complexities below the near surface section have been explained in chapter 1 in detail. The main producing interval is the Asmari formation (unit 4 in figure 4.2) that consists of carbonate rock. There is a clear difference in structural style between the horizons above this formation (post-Asmari interval) and the horizons below it (pre-Asmari interval).

## 5.2 Different travel time solutions

The Kirchhoff 3D prestack depth migration is performed in two steps. In the first step travel times are calculated and then at the second step migration is performed. The travel time computation methods have a considerable impact on the result of Kirchhoff prestack depth migration in complex geological cases. Two different algorithms have been tested. One is based on ray tracing and the second is solving the eikonal equation. In the first algorithm the actual ray path between two points has been tracked through the complex velocity model. The traveltime along the raypath is computed by integrating the velocity function along the ray. In the second method instead of tracing the rays, traveltimes are calculated from the equation that describes the change in traveltime as a function of location for a given velocity function. Two types of coordinate system have been used: rectangular and spherical. System. The spherical grid is closer to the geometry of a real wavefront and provides a better image. Four different types of travel time computation method have been tested as follows:

**Method 1** Ray tracing of the single arrival with minimum traveltime in a rectangular coordinate system: This travel time computation is in a rectangular grid and is based on Fermat's principle-the actual ray among several rays connecting two points (source and receiver at this case) is the one with minimum travel time (Meshbey, et al., 1996). The travel times of all these rays are calculated based on average slowness along each ray path. Then the minimum travel time assumption is applied to find the travel time of the selected ray. The accuracy of travel time computation is dependent on the thickness of the depth intervals chosen for ray tracing, the greater depth intervals imply a decrease in accuracy. In complex situations where the velocity varies both laterally and vertically it is better to select finer depth intervals for travel time computation. This is the fastest method among the four tested methods.

**Method 2**: ray tracing of the single arrival with the shortest path in a rectangular coordinate system: In most cases the direct ray is required by Kirchhoff migration. Sometimes the head wave arrives first and the direct ray is the one with shortest path and not minimum time. The problem of seismic depth imaging in complex media is characterized by the existence of triplications in ray tracing (Xu, et al., 1999) and as result multivalued travel times that put a limitation on single arrival travel time solvers (Geoltrain and Brac, 1993, Operto, et al., 2000, Xu and Lambare, 2004). The seismic forward modelling results in the Dezful embayment (chapter 2) show the triplications around the crest of the structure 'B' that is similar to Parsi and Karanj structures. Geoltrain and Brac, (1993) have shown the failure of using first arrival travel time in complex media. This failure is due to the fact that both secondary arrivals and associated amplitudes of those arrivals are not taken into account. The amplitude will be better preserved if the strongest arrival is selected in the migration (Audebert, et al., 1997, Thierry, et al., 1999). The best solution is to use the travel times of multiple arrivals (total ray-field information) and weight them by their amplitudes depending on the geometrical spreading and ray angles. This is a difficult task and is highly sensitive to errors in the velocity model. However using the single strongest arrival improves the migration (Thierry et al., 1999, Xu, et al., 1999, Operto et al., 2000). The use of the most energetic arrival is a reasonable alternative solution to multivalued travel time computation.

**Method 3**: eikonal-equation solver in a spherical coordinate system: In this method travel times are computed by solving the eikonal equation. Actually the travel time function is a solution to the eikonal equation (Cerveny, 2001):

$$(\nabla T)^2 = 1/c^2$$

This is a single arrival travel time solution and it can be either first arrival (minimum time) or the shortest path with the highest amplitude. The shortest path method has been tested in this study.

**Method 4:** ray tracing of first arrival in a spherical coordinate system: The spherical coordinate system in ray tracing is more time consuming than a Cartesian coordinate system but is closer to the real wavefront geometry.

## 5.3 Results from Parsi and Karanj 3D, Zagros FTB

The different travel time computations explained above have been tested on the 3D dataset from the Parsi and Karanj structures. The same interval velocity model has been used for all travel time solutions and the migration aperture for all migration tests was 300 inline and 300 crossline. In complex situations with steep dips the Kirchhoff migration for a given input seismic trace spacing is aliased. This generated some artefacts in the migrated image especially in the shallow section. Anti-alias filters are used to avoid generation of these artefacts. By using this filter migration can be performed with large apertures without degradation of data by aliasing noise.

There are a number of structural elements that can be looked at in the different migration results in order to verify how effective the methods are. Imaging the steep flanks of the structures in pre-Asmari interval, correct geometry of thrust surfaces, internal complex geometry of post-Asmari interval are issues that can be used to evaluate the goodness of prestack depth imaging results.

Figure 5.2a shows the migration result using a travel time solution based on Fermat's principle with rectangular coordinates (Method 1). This is the fastest travel time computation method and only the first arrival (minimum time) has been taken into account. The steep flank of the structure (southwest limb inside the circle) is missing. The upper picked reflector is the top of the pre-Asmari depth interval. The two reflectors picked in the southwest part of the section are the possible location for another deep anticline, but the events are not coherent enough to draw the complete picture of this deep small anticline. The geometry of the thrust fault between two anticlines is not clear enough. Figure 5.2b shows the same section but the selected single arrival is the one with minimum path (shortest path) rather than minimum travel time. The top Asmari reflector extends more towards the southwest (the upper green picked horizon to the right of the section). The structure located to the left that was not clear in the previous migration is better imaged. This result shows that for certain structures, such as steep flanks that have strong lateral velocity variations in the post-Asmari depth interval using the minimum travel time assumption is not right. The strongest arrival at this part of the structure is the one with shortest path, which passes through a low velocity interval right above the Asmari reflector in the post-Asmari depth interval. The reflectors focusing in the deeper part of the pre-Asmari depth interval (for example the lower picked horizon to the right of the section in figure 5.2b have also been enhanced with respect to the previous migration.

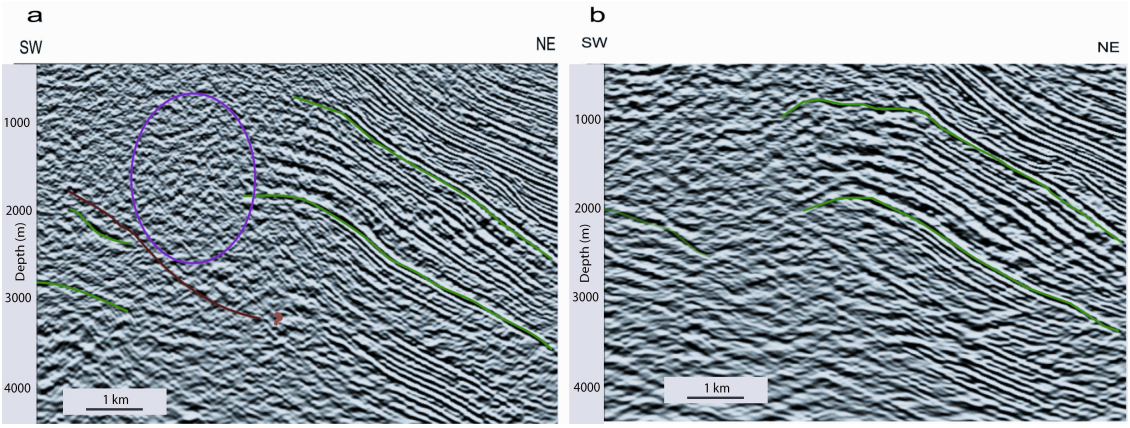


*Figure 5.2 PSDM results using Fermat's principle with rectangular coordinates for travel time computation a) minimum travel time, b) Shortest (minimum) path. The southern structure in the shortest path method is imaged better than minimum travel time method. The green horizon at the top is the Top Asmari reflector.*

Another example of the difference between first arrival based on minimum travel time (method 1) and shortest path (shortest path) is given in figure 5.3a and b. There are significant improvements in the focusing and image quality. The arrow shows the location of the deep structure. The thick overburden sequences with strong lateral heterogeneity make the correct imaging of this deep anticline very difficult. The improvement shown in figure 5.3b is remarkable. The structure can be picked with great confidence. The southern flank of the structure to the northeast is also imaged better with the shortest path travel time computation method (figure 5.3b). There are three structures shown in figure 5.3.b by the letters A (southern structure-Karanj), B (middle structure-Paranj) and C (northern structure-Parsi). The reflector packages above the middle structure in figure 5.3b (the yellow arrow) are an excellent well-focused reflector package from the post-Asmari interval.

The purple arrow in figure 5.3b shows the position of a thrust plane where southwest dipping beds are juxtaposed against northeast dipping beds. Figure 5.4a shows the results of travel time solution in a rectangular coordinate system based on Fermat's principle (method 2 explained above) and figure 5.4b shows the result of an eikonal solver for travel time computation (method 3). The picked horizons are drawn just to show the reflector continuity in the northern and middle structure. The upper green horizon is close to the top of the pre-Asmari interval. As has been stated earlier the poor quality of the images from the flanks led to two different thoughts among geologists and geophysicists (Motiei, 1995). Geologists believe that there should be continuous

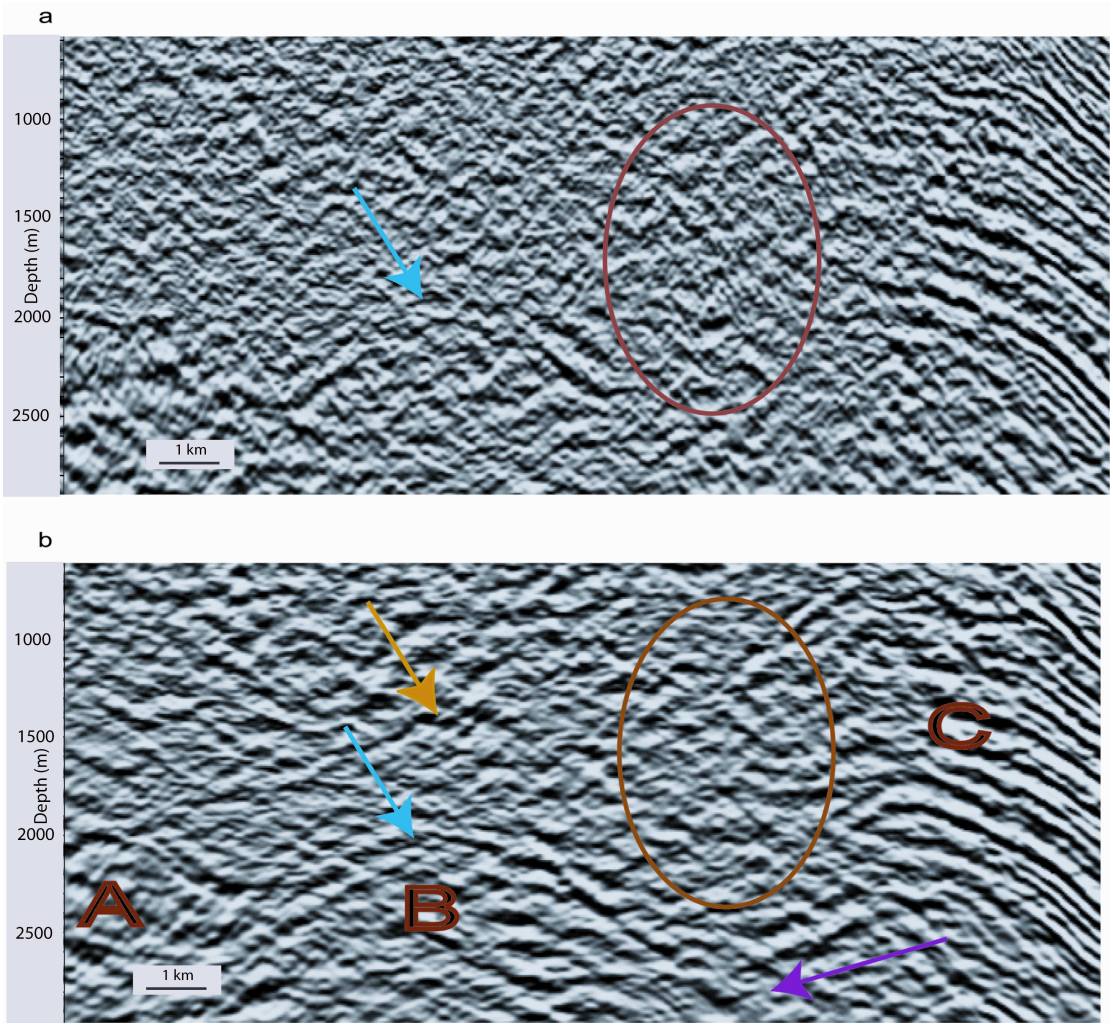


*Figure 5.3 The difference between first arrival based on minimum travel time (a) and minimum path (b). The blue arrow shows the location of deep structure. The shortest path method gives clear image of the structure. The yellow arrow shows the improved focusing in the overburden interval. The purple arrow shows the position of a thrust plane where southwest dipping beds are juxtaposed against northeast dipping beds.*

structures with steep to overturned dip while geophysicists put a reverse fault in the flanks of the structures. Figure 5.4b shows that the southern flank of the northern structure at the location of this inline is continuous and there is no evidence of reverse faulting in the flank. The thrust fault between the northern structure and the middle structure is also well focused.

The results of the fourth travel time computation (Fermat's principle in a spherical coordinate system) show better focusing and imaging compared with the 3 previous methods applied. Figure 5.5a and b show a comparison between the eikonal solver (method 3) and the spherical Fermat (method 4). The southern flank of northern structure in figure 5.5b (spherical Fermat) is extended more than in figure 5.5a (eikonal solver).

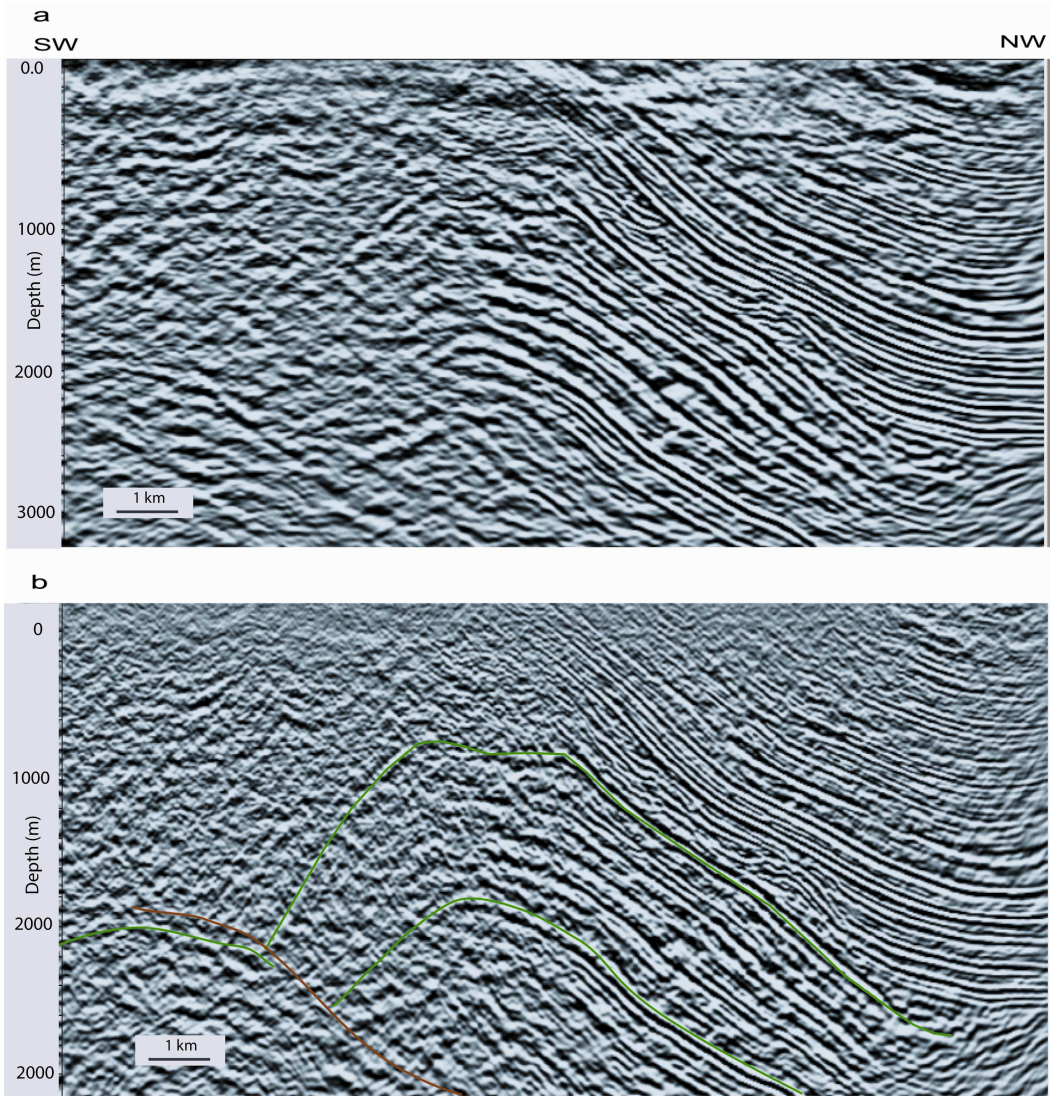


*Figure 5.4 a) PSDM results using Fermat's principle with rectangular coordinates (shortest path) and b) the result of an eikonal solver for travel time computation. The picked horizons are drawn just to show the reflector continuity in the structures. The upper green horizon is close to the Top Asmari. The trough has been picked so the peak can be followed. The southern flank of the northern structure (Parsi) is continuously imaged. Without introducing any fault the flanks of the structure can be picked.*

The arrows to the right of figure 5.5a and b show the improved imaging/focusing in the post-Asmari (overburden) interval with a spherical Fermat's travel time solution. Figure 5.6 is a 3D slice of the migrated data with a spherical Fermat travel time solution and it shows the clear image from the flanks of the northern structure both in cross section and depth slice view. In complex situations where the seismic migration objectives are to obtain a geologically consistent image seismic imaging is essentially interpretive (Lines, et al., 2000). Actually this prestack depth imaging is interpretation based so the results of migration is not only being evaluated by processing based methods such as common image gather quality check or stack quality control but also a comprehensive interpretation has been done to verify the results of depth migration.

The information from more than 90 well was included in the analysis. This study clearly shows that by incorporating detailed geologic interpretation, the single arrival Kirchhoff prestack

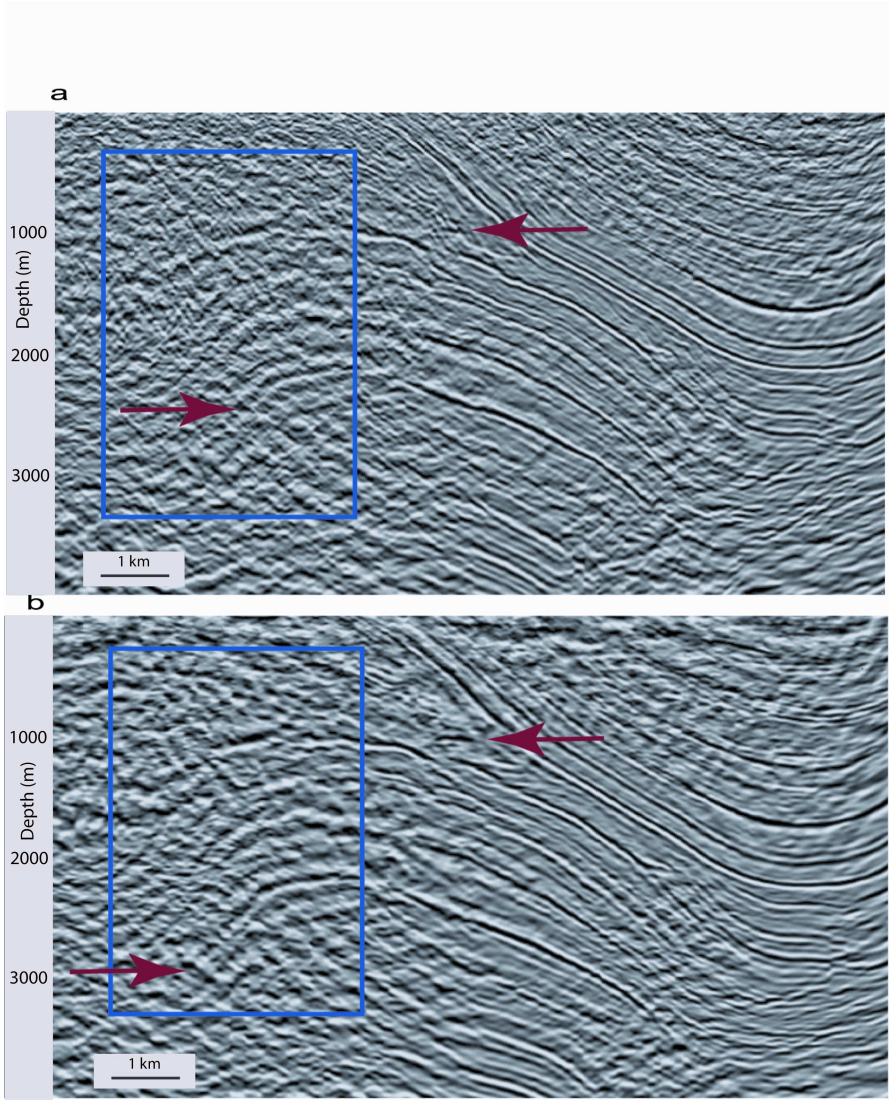


*Figure 5.5.Comparison between a) the eikonal solver (method 3) and b) the spherical Fermat (method 4). The southern flank of northern structure in figure 5.5b (spherical Fermat) is extended more than in figure 5.5a (eikonal solver). The arrows to the right of figure 5.5a and b show the improved imaging in the post-Asmari (overburden) interval with spherical Fermat's travel time solution.*

depth migration gives excellent results. By constraining the single arrival Kirchhoff PSDM with hard geological information I achieved results that are significantly more useable than by unconstrained PSDM alone. The results also show that the spherical coordinate system for travel time calculation gives better results than rectangular coordinate system. Around the flanks of folds with very steep limbs selecting the single arrival with shortest path rather than minimum arrival time gives better focusing than minimum time arrival.

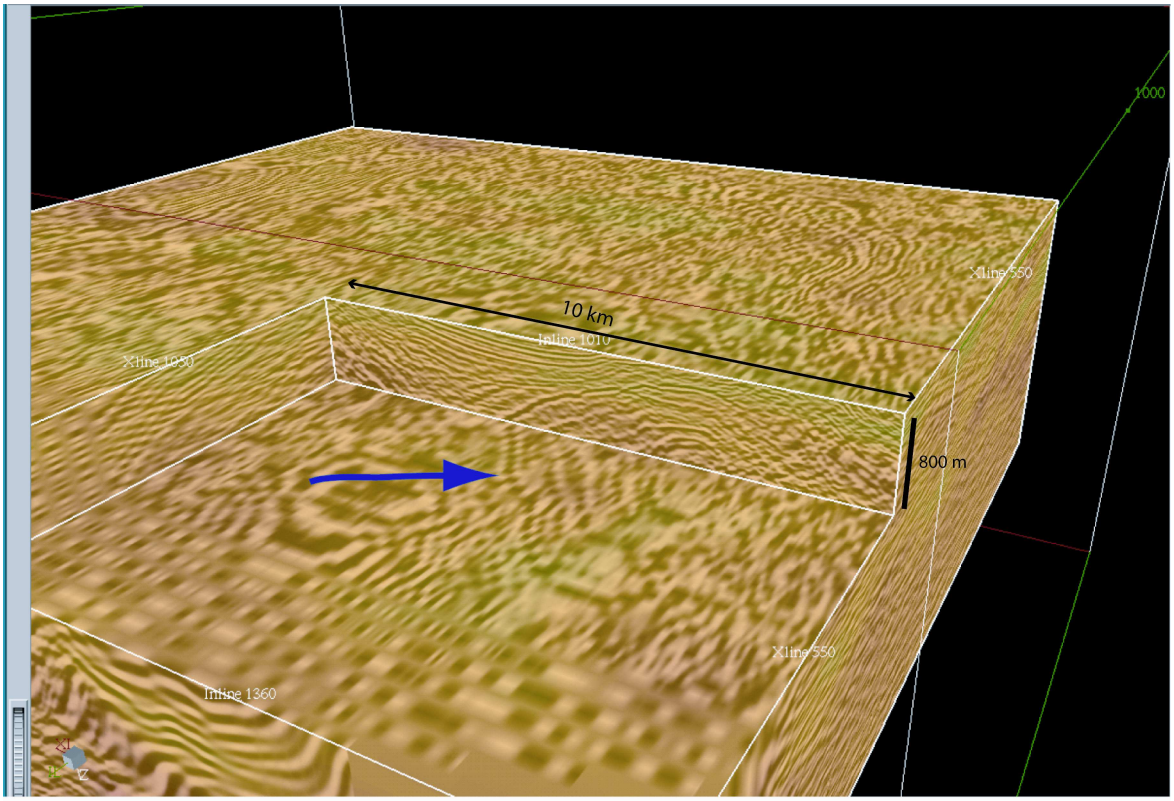


*Figure 5.6 3D volume of the migrated data with a spherical Fermat travel time solution (method 4). It shows the clear image from the flanks of the northern structure both in cross section and depth slice view.*

# 6 Detailed geological modelling and finite difference forward realization of a 2D regional section from the Dezful embayment of Zagros FTB

## 6.1 Role of Modelling

There are a number of strategies for building geological models (e.g. Bryant, and Flint, 1993, Petersen, 1999, 2004, Fagin, 1999, Patel and McMechan, 2003). Any successful geological model must include both sedimentary related architecture (facies) and structural elements (for example faults and folds). Seismic modelling describes the forward process of propagating waves from sources to scatterers down in the subsurface and back to the receivers. It is the numerical computation of synthetic seismograms for a given geologic model of the subsurface (Santos, et al., 2000, Gray, et al., 2001, Krebes, 2004). In advanced modelling, the model units (geological units or structural elements) follow the genetic significance. They not only represent the simple geometry but also represent the sequence of geological events. A subsurface model that satisfies more than one set of observations (Petersen, 2004) is ideal for modelling purposes. In the Zagros FTB there are several complexities such as near surface related problems (severe topographic variation and static complications), complex folding, intense faulting and different structural style between the geologic units exposed at surface and the subsurface structures. These made the seismic acquisition, processing and also interpretation a difficult task.

In such complex cases seismic modelling are useful for better acquisition design, improved processing sequences and reliable interpretation. It is useful in a wide range of applications in exploration seismology. In seismic acquisition, seismic forward modelling reduces the risk of seismic exploration by providing quantitative information to design better 3D surveys (Gain, et al., 1998). Illumination tests can be performed to obtain the best acquisition geometry in complex areas with poor illumination. In complex situations such as the Zagros FTB seismic acquisition has some difficulties in dealing with problems such as illumination and noise. By building a complex model and forward realization, different attributes (for example, arrival time, angle of incidence, and amplitude) can be collected and the acquisition optimized.

Seismic modelling can be used in seismic processing and interpretation to optimize the processing sequences and check the validity of interpretation particularly in complex situations. An important role of seismic modelling is to calibrate migration methods (Gray et al., 2001). For example the Marmousi 2D model (Versteeg, 1994) that was generated by the French Petroleum Institute has been used for testing migration and velocity estimation methods.

Edwards, (1978) recommended the use of seismic modelling to the Oil Service Company of Iran (OSCO). He stated that the company's special studies group in support of interpretation projects could arrange and carry out interval velocity studies for modelling purposes. He also mentioned that the interpretation staff should model their seismic and well data in areas where wells are located nearby. Nevertheless modelling has not been taken into account in the Zagros FTB for many years and I believe there are possibilities that seismic modelling can improve seismic data acquisition, processing and interpretation in this area. This is a first step although it comes rather late.

## 6.2 COMPOUND Model Building of the Dezful embayment regional section

One of the common problems in model building for structures in thrust and fold belts is complex internal geometry of the structures. Morse, et al., (1991) have modelled fault-related folds and analyzed the seismic unmigrated and migrated response. Sukaramongkol, (1993) has applied seismic forward modelling on a non-emergent thrust front in the Fallen Timber Creek area, southern Alberta foothills, and compared the results with the real seismic data. Johansen, et al., (1994) have modelled an outcrop analogue from imbricate fault-bend folds with steep forelimbs at the frontal part of the west Spitsbergen fold and thrust belt. Interface based model building and cell based model building approaches have been used to define the models (e.g. Fagin, 1991, Kirtland Grech, et al., 1997, Petersen, 1999, 2003, Bryant and Flint, 1993). The geological units are building blocks of the model and faults planes have been defined as either discrete planes or as the boundary between hanging wall and footwall blocks. In cell based or grid based representation (Bryant and Flint, 1993, Petersen, 1999, 2004, Patel and McMechan, 2003) the curves or surfaces are used to define the geometry of a complex model.

In this study a 2D regional cross section from the Iranian Zagros FTB has been used for modelling with a shared earth strategy (Petersen, 2004). A finite difference realization has been applied to generate a number of shots around the complex structures to investigate the possibility of improving acquisition design and processing sequences.

The integration of different data types for model definition in space and time is increasing. A commonly applied strategy for modelling clastic reservoirs has been explained by Bryant and Flint, (1993). It includes five major steps: definition of the space occupied by the modelled interval; recognition of geological units within the model space; assignment of geometries to the units; arrangement of the units within the model space (architecture); assignment of properties to the units. Patel and McMechan, (2003) used well log data and control horizons to build a girded model of physical properties such as seismic velocity. Inverse distance weighting or linear

interpolation has been used to extend the well log information into the 2D model. The method has been applied to build a model from an overthrust model of western Canada.

Petersen, (1999) proposed a modelling approach -COMPOUND model- to construct shared earth models. I have applied this approach on the same regional 2D section that has been used for ray-based modelling (chapter2). The COMPOUND model is composed of compound cells and each cell occupies an area. Different physical property distributions are assigned to each cell. The cell hierarchy relates localized property distributions to each other in space. The model is consistent with the geological evolution since the final distribution of properties is the result of geological processes over time. In complex structural models where the sequence of events is important this possibility of COMPOUND modelling makes it possible to differentiate between different stages of deformation (faulting, folding or fault-related folding, erosion, etc.). If for example the result of a geological process such as a deformation phase, orogenic event or a sedimentation related process is overprinted by the result of another process, the properties belonging to the latest (in 'time') stage replace the previous one for a specific position in 'space'. This ensures the time and space consistency of the geological model. The geometry is controlled by curves of parametric description and properties by 1D function.

The property distribution in space is defined by property cells (P cells). The curves defining geometry and the property function are combined together in a P cell. The characteristics of the P cells are: the curve, the property values, and curve orientation. Sedimentary bodies are rarely equidimensioanl so for proper requires modelling knowledge of the orientation of the geological units. It is possible with curves and the hierarchy approach in COMPOUND to build any kind of internal geometry and orientation such as truncations, onlap, downlap, and complex small scale faulting and folding inside the geologic units.

The selected cross section has been built based on all available information including 2D seismic profiles, well information and surface geology data from outcrops. The section has been restored and balanced (Mapstone, 1978). Figure 1.5 shows the location of the line in the Zagros FTB. It crosses exposed anticlines in the northern part and deeply buried anticlines covered by recent sediments in the southern part. Therefore the reservoir horizons in the south are exposed at the surface further north. Figure 6.1 shows the cross section as it has been drawn by Mapstone, (1978). The seismic data in addition to usual geological well and surfaces data was used extensively in elucidating subsurface structure. The dimension of studied regional model is 81kmx17km.

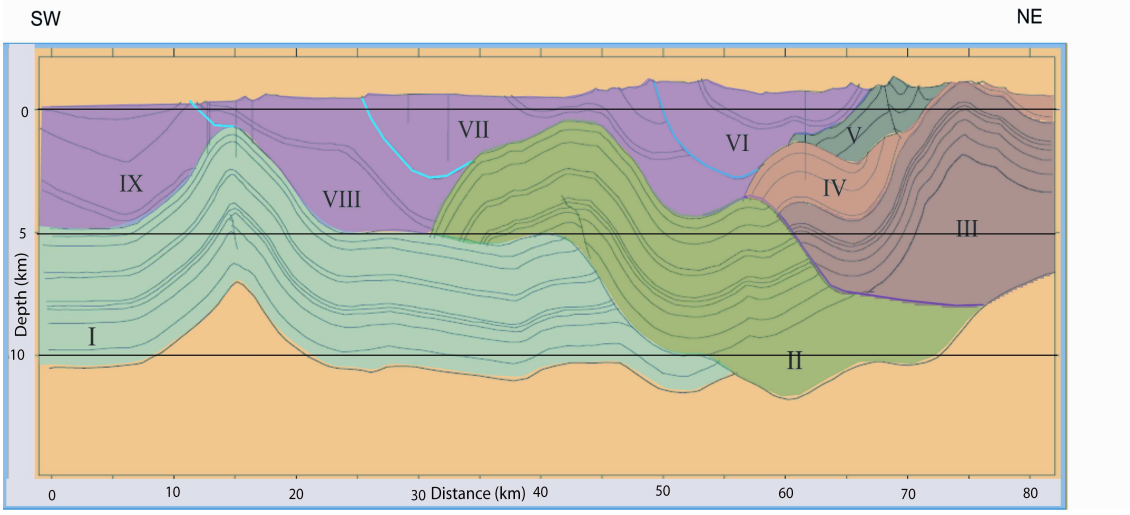


*Figure 6.1 The regional structural cross section from the Dezful embayment of the Zagros FTB. The section originally constructed and balanced by Mapstone, (1978). The numbers refer to units defined in the hierarchical modelling strategy used in the study.*

The section has been divided into 9 main building blocks. This is structurally consistent with the deformation history of the area crossed by the section. An important parameter in the Zagros FTB is the detachment level in the basal part of the Gachsaran formation that cause disharmony in deformation style of the intervals above the detachment (post-Asmari formations) with the rock units below (pre-Asmari formations). Units VI, VII, VIII, and IX in figure 6.1 represent the post-Asmari interval or overburden. The units I to V represent the competent pre-Asmari interval. The thrust faults at boundary of units I, II, III, IV, and V show a sequence of thrusting from northeast to southwest. The dip of thrust decreases from northeast to southwest and this is an indication of the development of thrusts in the footwall of the existing thrusts. The boundary between units III and IV is another detachment level. The two thrusts in unit V flatten in this detachment level. So the tree like hierarchical model building strategy in COMPOUND makes it possible to construct the regional framework of the profile completely consistent with the structural evolution of the area. Deformation in unit III overprints the deformation in unit II and deformation of unit II overprints the deformation in unit I. The deformation in the overburden (units VI to IX) is separated from deeper competent intervals and is younger than them.

The displacement distribution (from zero to maximum displacement) of faults inside each unit is organized by the curves and cell arrangement. It is possible to build different fault-related folding models by this method. The exact location of fault displacement vectors is controlled by the curves.

## 6.3 Gachsaran formation-modelling the internal complexity

After building the main mega-building blocks of the model the next attempt is to include the internal structural and stratigraphic detail in each unit. The overburden section (units VI to IX in figure 6.1) includes significant heterogeneity in structure and also rock types. The internal geometry of the Gachsaran formation (lower part of the overburden) shows significant variation from place to place. It is divided into seven members (Silinger and Crighton, 1959). The formation consists of alternating salt, anhydrite (gypsum at or near the surface), limestone, marl and shale (Favre, 1974). The formation shows great variation in thickness from well to well, particularly from crest to the flanks of the structures. A representative section was introduced by Oswald, (1978) with a total thickness of 1564.5m. The variations of thickness can be ascribed to the following causes:

1- changes in bedding attitude;
2- normal faulting;
3- thrust faulting, contraction and parasitic folding; and
4-depositional thickness changes (Oswald, 1978).

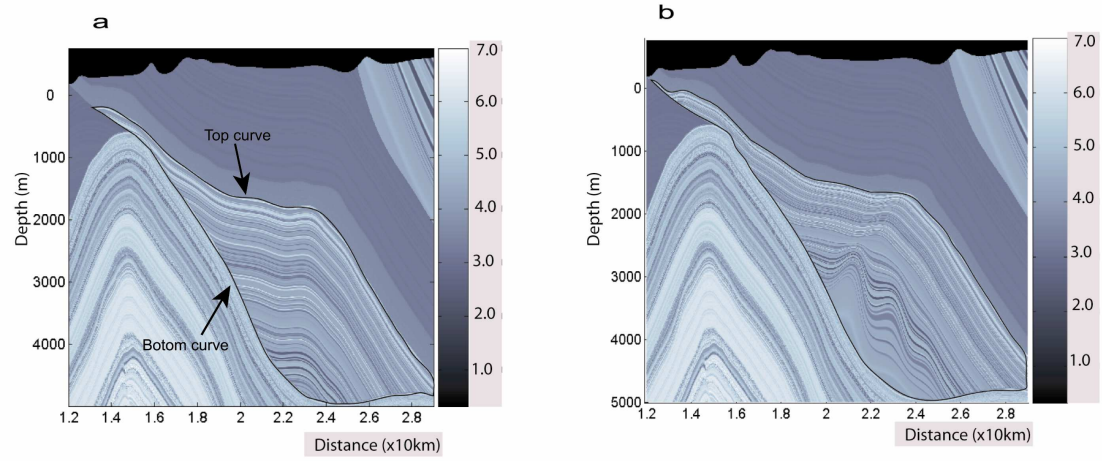


*Figure 6.2 Detail modelling of unit VIII (Figure 6.1). a) Modelling results before detail internal geometry definition. The internal geometry is parallel to the curve representing unit top and truncated by the curve representing the bottom of the unit. b) Modelling results after detailed internal geometry definition. Parallel bedding at the upper part of the unit, squeezing and thickening at the middle part, and onlap geometry at the lower part are included in the model. The colour represents the scaled acoustic impedance.*

Members VI and VII at the top of Gachsaran formation show more uniformity in thickness than the lower members. Around the southern edge of the studied profile the onlap geometry has already been reported (Oswald, 1978) for the lower members of the formation while for member IV, that is the main salt unit, salt moves from anticlines to adjacent synclines. The depositional

differences in thickness continued until member V. Syn-sedimentary folding also reported in the Gachsaran formation further to the south of the studied profile (Sherkati and Letouzey, 2004).

For modelling purposes the members of the Gachsaran formation have been included in the model and thickness variation at each location has been defined based on the possible causes explained above. For members II and III in the flanks of structures, onlap orientation has been built, for member IV thickness variation was modelled as plastic behaviour of salt and the upper members were kept more or less uniform in between the wells. A good example of application of all these geological facts for Gachsaran formation is in unit VIII. With COMPOUND modelling it is possible to define onlap geometry, truncation, squeezing and thickening proportionally. Therefore all the geometries that have been reported from the Gachsaran formation can be easily included in the model. Figure 6.2a and b shows the final detailed modelling of unit VIII. The colour in the figure represents the scaled acoustic impedance. The impedance variation in the whole depth range (17 km) is large so using the original impedance values we will not be able to chase the detail. So for display purpose I have scaled the acoustic impedance. Therefore it is possible to distinguish the fine variations in the overburden at the same time follow the detail variations in the deeper part of the section. In figure6.2a the area inside the black line (unit VIII) is modelled by using three curves. A top curve, that is parallel to the geometry of the upper part of unit VIII. A lower curve that is parallel to the top curve and finally a controlling curve parallel to the top of unit I that is below unit VIII. This curve causes truncation of all uniform internal layering of unit VIII (Figure 6.2a). Figure 6.2b shows the results of detailed modelling for the same unit. The unit has been divided into six smaller units representing the members of Gachsaran formation (The lowest member, member 1, is a competent interval has been modelled as the topmost part of unit I). Onlap geometry has been defined for members 2 and 3. Thickening and squeezing have been included in the modelling of member 4. This interval is the main salt interval in the Gachsaran formation with great variation in thickness because of the high degree of incompetency exhibited during folding (Oswald, 1978).

Figure 6.3 shows the final model after putting all detail in the model, which includes the regional structural framework as well as small-scale stratigraphic detail. Slowness and density are the main properties included in the model. The sonic logs and formation density logs were used to define the slowness and density variation in each cell of the model. In cases where there is no sonic log available (for the upper part of overburden and very deep rock units) the velocity function was derived from check shot surveys. A lithology dependent sonic-density relationship has been used to obtain density values for intervals where there was no density log available. The grid spacing is 12.5mx5m.

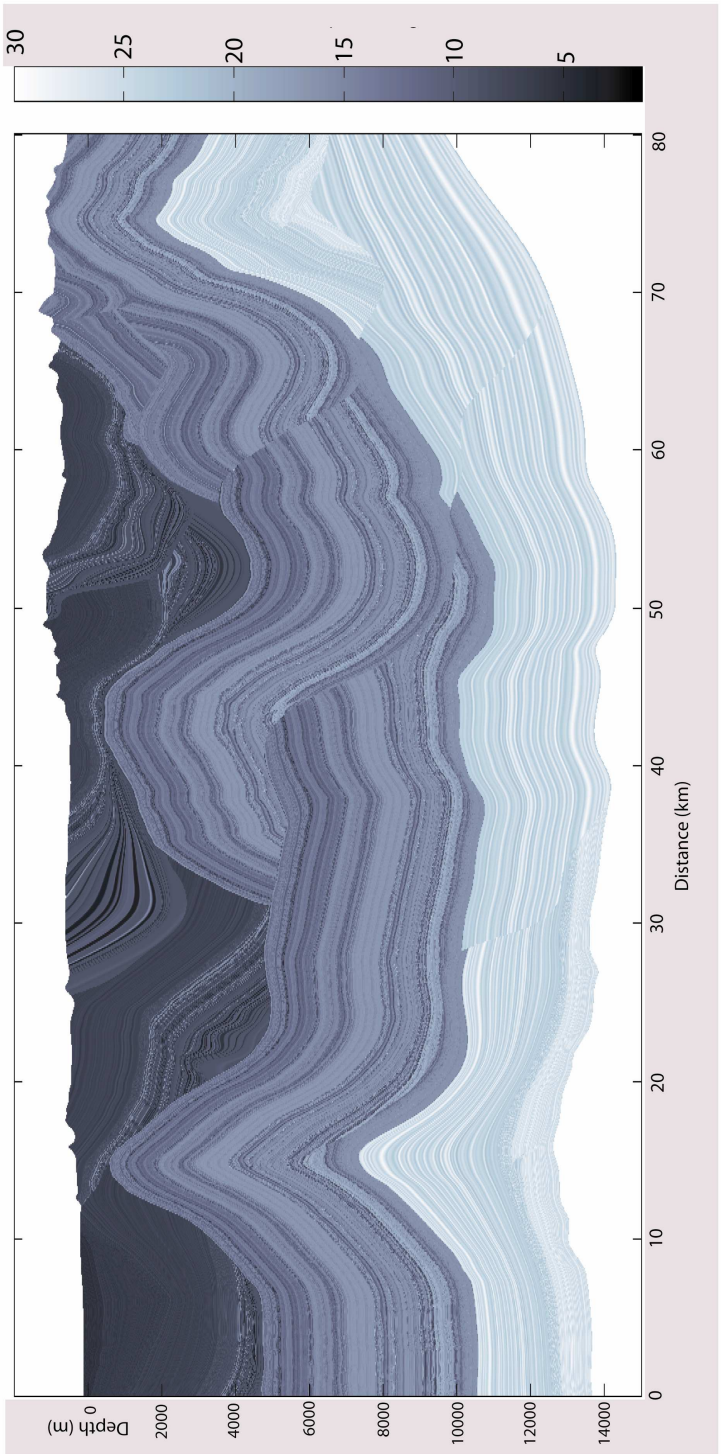


*Figure 6.3 The final model. It includes regional structural elements as well as small-scale stratigraphic detail. The colour represents the scaled acoustic impedance.*

## 6.4 Finite difference forward realization

Finite difference forward modelling code has been used to generate a number of shots. First shot is located in the northeast flank of the anticline of unit 1 at x=20000m (figure 6.1). Two different model geometries have been used with the same velocity model (figure 6.2a and b). Geological detail of the Gachsaran formation was honoured in the detailed model (figure 6.2b) while in the regional model the whole formation was modelled with uniform internal geometry. The main purpose of shooting at this location (x=20000m figure 6.1) is first to see the effect of thick overburden on the seismic wave field. The second objective is to compare the seismic response of detailed geometrical modelling (figure 6.2b) with regional geometrical modelling (figure 6.2a). A split-spread source/receiver array has been. Figure 6.4 shows a snapshot of the propagated seismic wavefield after 0.9 s for both models. The events called 'A' in the regional model (Figure 6.4a) are the reflections from the boundary between unit I and unit VIII. The events called 'B' (Figure 6.4b) are the reflections from the internal parts of the unit VIII. These events are parallel representing parallel bedding defined in the regional model (Figure 6.2a). The same events ('B') in the detailed model response (figure 6.4b) are not parallel and reflect the internal complex geometry of unit VIII. Figure 6.5a and b show the common shot gather for the two shots. It is clear that the seismic wave field in the detailed model (figure 6.5b) is more complex than the regional model response. Diffractions shown inside the rectangle in figure 6.5b are due to the complex geometry of salt beds of the Gachsaran formation (member 4). This single shot in the flank of the anticline located in unit I shows how the correct modelling of overburden geology affects the seismic response.

It is recommended to build such regional-detailed models across the Zagros FTB (controlled by seismic interpretation and well information) in order to understand the seismic wavefield behaviour at different thrusted folds with complex overburden velocity structure.

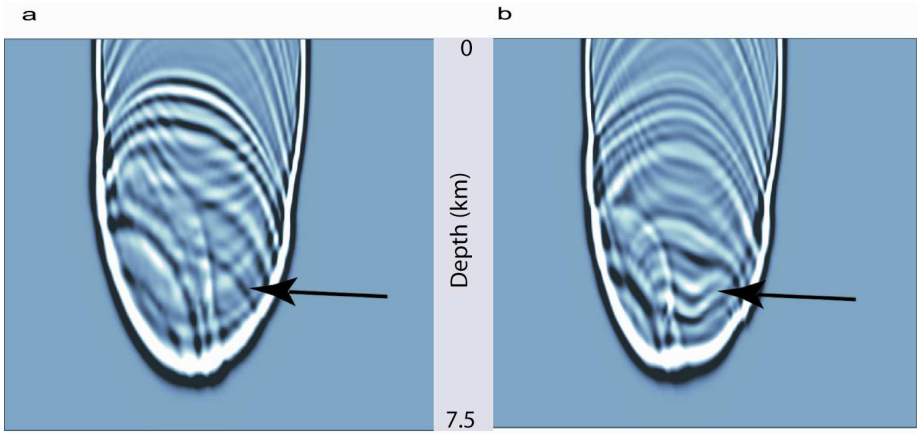


*Figure 6.4 Snapshots from a shot located at the northern flank of the unit I (figure 6.1 x=20000) anticline from two models shown in figure 6.2 after 1.1s. a) Response from regional model shown in figure 6.2a. b) Response from detailed model shown in figure 6.2b. The results are different.*

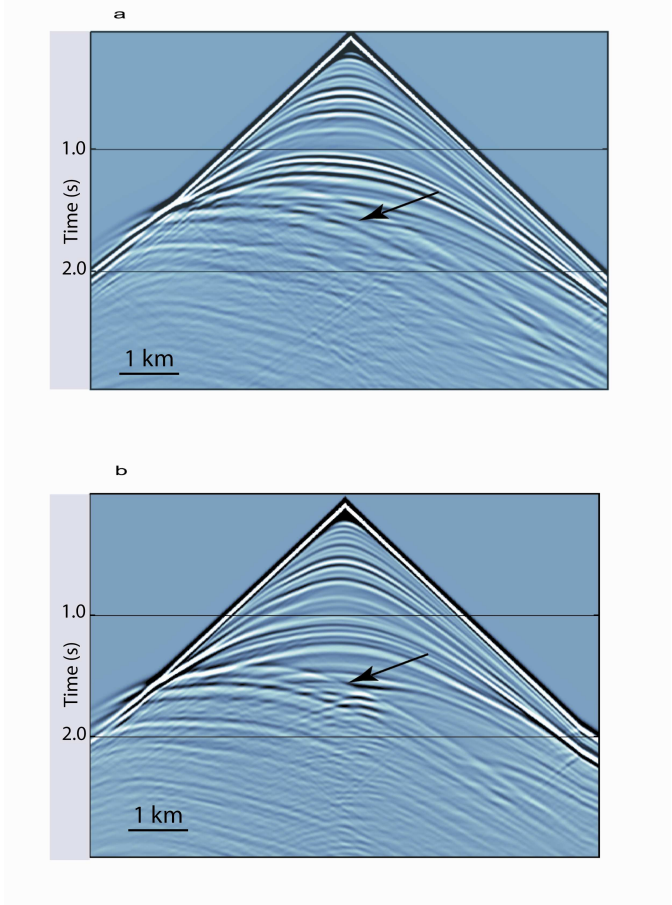


*Figure 6.5 Common shot gather results of the shots located in the northern flank of the anticline in unit I (figure 6.1, x=20000). A) The common shot gather of model shown in figure 6.2a. b) The common shot gather of model shown in figure 6.2b.*

# 7 Conclusion

The ultimate goal of seismic data processing is to recover an image of the subsurface geological structure. In this dissertation seismic forward modelling (asymptotic and finite difference), a hybrid migration velocity analysis and prestack depth migration algorithms have been applied to analyze complex fold and thrust belts with strong topographic variations.

In mountainous areas such as the Iranian Zagros FTB that has structural complexities seismic forward modelling is a useful tool to help in all steps of seismic study including acquisition, processing and interpretation. Since this is the first time seismic forward modelling is applied to the fault related folds in the Iranian Zagros FTB, the results show the necessity of modelling itself for the area of study, as well as the need to plan more detailed modelling studies. Structures are complex and velocity does not have a simple gradient, but changes laterally and there is also some velocity inversion, so special processing procedures, such as Prestack Depth Migration, are becoming more important, and for such imaging methods modelling is essential.

Asymptotic forward modelling results show

- The conventional velocity analysis does not produce correct images and simple calibration with wells especially in high velocity carbonates considerably improves the image quality.

- Non-hyperbolic events have been identified in the shot gather modelling. In order to obtain the correct image and include these events in the processing only prestack imaging methods should be applied.

- The ray coverage is not sufficient in steeply faulted flanks of structures and in places with thick overburden (with strong lateral velocity variation) so other seismic modelling methods such as finite difference methods should be tested.

Detail geological models have been built with the COMPOUND model builder.

- This type of model building honours the geological detail as well as structural elements. Regional and small-scale detail is included in the model. The generated model is very close to the real geology.

- The seismic response of such model reflects the internal geometry of the geologic structures and facies. Finite difference shot gather modelling of the detail model shows the complexity of the seismic wave field generated by the thick overburden.

For migration velocity analysis a model-based hybrid tomographic strategy has been introduced. The proposed procedure is based on tomography of common image gathers and has 4 main stages, initial model generation, regional velocity update, detailed high-resolution velocity update and final model generation.

- It has the advantage of seismic interpretation at different stages of the velocity analysis, Well information is included in the procedure from the beginning,

- The procedure can confidently be expected to converge to the right answer, because the updates of each stage are reflected in the partial prestack depth migration and controlled by hard geological information from wells,

- The results of migration velocity analysis were promising and provide much better focusing. The final interval velocity model was structurally consistent and reflects the lithological changes as well.

The different single arrival Kirchhoff prestack depth migration tests clearly show that by incorporating detailed geological interpretation, the single arrival Kirchhoff prestack depth migration gives excellent results.

- By constraining the single arrival Kirchhoff PSDM with hard geological information I achieved results that are significantly more usable than by unconstrained PSDM alone.

- The results also show that the spherical coordinate system for travel time calculation gives better results than rectangular coordinate system.

- Around the flanks of folds with very steep limbs selecting the single arrival with shortest path rather than minimum arrival time gives better focusing than minimum time arrival.

# References

Al-Yahya K., 1989. Velocity analysis by iterative profile migration. Geophysics, 54, 718–729.

Anselmetti, F., and G. P. Eberli, 2001. Sonic velocity in carbonates- A combined product of depositional lithology and diagenetic alterations. SEPM Special publication No. 70, 193-216.

Anselmetti, F., and G. P. Eberli, 1993. Controls on sonic velocity in Carbonates. Pure and Applied Geophysics, 141, 287-323.

Audebert, F., D. Nichols, T. Redkal, B. Biondi, D. E. Lumley, and H. Urdaneta, 1997. Imaging complex geologic structure with single-arrival Kirchhoff prestack depth Migration. Geophysics, vol. 62, 1533-1543.

Bally, A.W., 1983. Seismic expression of structural styles, volume 3 Tectonics of Compressional provinces/strike slip tectonics. AAPG Studies in Geology series no.15.

BGP, 2002. Final Acquisition report of Karanj & Parsi 3D survey for National Iranian Oil Company.

Biondi, B., 2004. 3D seismic imaging, Stanford Exploration Project. 356pp.

Bishop, T. N., Bube, K. P., Cutler, R. T., Langan, R.T., Love, P. L., Resnick, J. R., Shrey, R. T., D. A. Spindler, and H. W. Wyld, 1985. Tomographic determination of velocity and depth in laterally varying media. Geophysics, 50, 903-923.

Bryant, I. D., and S. S. Flint, 1993. Quantitative clastic reservoir modelling: problems and Perspectives. Spec. Pubs int. Ass. Sediment. 15, 3-20.

Carcione, J.M., Herman, G.C. and ten Kroode, A.P.E., 2002. Seismic modelling. Geophysics, vol. 67, 1304-1325.

Ćervenŷ, V., 2001. Seismic Ray Theory. Cambridge University Press, 713pp.

CGG, 2003. Final report Seismic data processing Karanj and Parsi 3D IRAN.

Clapp, R. G., B. Biondi, and J. F. Claerbout, 2004. Incorporating geologic information into reflection tomography. Geophysics, 69, 533-546.

Claerbout, J. F., 1985. Imaging the Earth's interior, Blackwell Scientific Publications.

Cox, M., 1999. Static corrections for seismic reflection survey, Soc. Explo. Geophys.

Dell'Aversana, P., D. Colombo, M. Buia, and S. Morandi, 2003. Velocity/Interface model building in a thrust belt by tomographic inversion of global offset seismic data. Geophysical prospecting, 51, 23-35.

Docherty, P., 1991. A brief comparison of some Kirchhoff integral formulas for migration and inversion. Geophysics, 56, 1164-1169.

Edwards, R. V., 1978. Review of OSCO's seismic data processing. Oil Service Company of Iran, Internal report no. 1287.

Etgen, J., 1990. Residual Prestack migration and interval velocity estimation, Ph.D. thesis, Stanford University.

Fagin, S. W., 1991. Seismic Modelling of Geologic Structures, Applications to Exploration Problems, Geophysical Development series, no.2, Society of Exploration Geophysicists

Fagin, S. W., 1999. Model-Based Depth Imaging. Course Notes Series, No. 10, Society of Exploration Geophysicists, 173pp.

Farmer, P., Gray, S., Hodgkiss, G., Pieprzak, A., Ratcliff, D. and Whitcombe, D., 1993. Structural imaging,

Toward a sharper subsurface view. Oilfield Review, 5, 28-41.

Favre, G, 1974. The post Asmari formations of south IRAN. Oil Service Company of Iran, Internal report no. 1220.

Favre, G, 1975. Structures in the Zagros Orogenic Belt. Oil Service Company of Iran Internal report, number 1233.

Faye, J. P., and J. P. Jeannot, 1986. prestack migration velocities from focusing depth Analysis. 56th Ann. Internat. Mtg., Soc. Expl. Geophys., Expanded abstracts, 438-440.

French, W.S., 1975. Computer migration of oblique seismic reflection profiles. Geophysics, 40, 961-980.

Gain, G., G. Cambois, M. Gehin, and R. Hall, 1998. Reducing risk in seismic acquisition and interpretation of complex targets using a Gocad-based 3D modelling tool. SEG Expanded Abstracts.

Geoltrain, J., and S. Brac, 1993. Can we image complex structures with first arrival travel-time? Geophysics, 58, 564-575.

Gray, H. S., J. Etgen, J. Dellinger, and D. Whitmore, 2001. Seismic migration problems and solutions. Geophysics, 66, 1622-1640.

Gray, S. H., 2000. Interpretive seismic imaging in structurally complex areas. In Depth imaging of Foothills seismic data, Canadian Society of Exploration Geophysicists, 106-107.

Huber, H., 1976. Tectonic map of south-west of Iran, 1:2500000. National Iranian Oil Company, Exploration and Production.

Gray, S. H., and K. J. Marfurt, 1995. Migration from topography, improving the near-surface image. Can. Soc. Explo. Geophys., 31, 18-24.

Gray, S. H., S. Cheadle, R. Vestrum, J. Gittins, T. Zhu, and H. Nanan, 2002. Using Advanced seismic imaging tools to see the invisible beneath foothills structures. CSEG Recorder, vol 27, March 16-28.

Hubral, P., 1977. Time migration - Some ray theoretical aspects. Geophysical Prospecting, 25, 738-745.

Jensen, S. L. D. Hunt, and S.A. Petersen, 2004. Seismic modelling of sulphate dissolution and karts collapse related deformation. EAGE 66th Conference and Exhibition, Paris.

Johansen, E. S., S. Kibsgaard, A. Andresen, T. Henningsen, and J. R. Granli, 1994. Seismic modelling of a strongly Emergent Thrust Front, West Spitsbergen Fold Belt, Svalbard. The American Association of Petroleum Geologists Bulletin, v. 78, p. 018-1027.

Jones, P., 1982. Quantitative Geometry of Thrust and Fold Belt Structures. AAPG, 26pp.

Kirtland Grech, M. G., D. C. Lawton, and D. A. Spratt, 1999. Numerical Seismic modelling of fault-fold structures in a mountainous setting. CSEG Ann. Mtg., Expanded Abstracts, 22-26.

Koren, Z., D. Kosloff, U. Zackhem, and S. Fagin, 1999. velocity model determination by tomography of depth migrated gathers. In Model-based depth imaging, Course Notes Series, No. 10, Society of Exploration Geophysicists.

Kosloff, D., J. Sherwood, Z., Koren, E. Machet, and Y. Falkovitz, 1996. Velocity and interface depth determination by tomography of depth migrated gathers. Geophysics, 61, 1511-1523.

Krebes, E. S., 2004. Seismic Forward Modelling. CSEG Recorder, Vol. 3, April 2004, pp 28-39.

Larner, K. L., L. Hatton, B. S. Gibson, and I. C. Hsu, 1981. Depth migration of imaged time sections. Geophysics, 46, 734-750.

Lines, L., W. Wu, H. Lu, A. Burton, and J. Zhu, 1996. Migration from topography: Experience with an

Alberta Foothills data set. Can. J. Explo. Geophys., 32, 24-30.

Lines, L.R., S. H. Gray and D.C Lawton, 2000. Depth imaging of Foothills seismic data. Canadian Society of Exploration Geophysicists, 275pp.

Lingrey, S., 1991. Seismic modelling of an Imbricate Thrust Structure from the Foothills of the Canadian Rocky Mountains. in Fagin, S.W., ed., Seismic Modelling of Geologic Structures Applications to exploration Problems, Geophysical Development, no.2, Society of Exploration Geophysicists, p.111-125.

Mapstone, N. B., 1978. Structural geology of structures of Dezful (north) Embayment. Oil Service Company of Iran (internal report, Technical note 13/1978).

Meshbey, V., D. Kosloff, Y. Rogoza, O. Meshbey, U. Egozy and J. Cozens, 1996. A method for computing travel times for an arbitrary velocity model. 66th Ann. Internat. Mtg., Soc. Explor. Geophys., Expanded abstracts, p523-526.

Mitra, S. and Mount, V.S., 1998. Foreland Basement-Involved Structures. AAPG Bull., 82, 70-109.

Mitra, S. and Fisher, G.W., 1992. Structural Geology of Fold and Thrust Belts. The John Hopkins University Press, Baltimore, 254 pp.

Morse, P. F., G. W. Purnell, and D. A. Medwedeff, 1991. Seismic modelling of Fault-related Folds, in Fagin, S.W., ed., Seismic Modelling of Geologic Structures Applications to exploration Problems, Geophysical Development, no.2, Society of Exploration Geophysicists, p. 127-152.

Motiei, H, 1995. Petroleum geology of Zagros-1. Geological Survey of Iran (in Persian), 589pp.

Operto, S., S. Xu, and G. Lambare, 2000. Can we image quantitatively complex models with rays? Geophysics, 65, 1223-1238.

Oswald, D. H., 1978. The Gachsaran formation of Gachsaran field. Oil Service Company of Iran, report No. 1281 (Internal report).

Patel, M. D., and G. A. McMechan, 2003. Building 2-D stratigraphic and structure models from well log data and control horizons. Computers and Geosciences 29, 557-567.

Pattinson, R., and M. Takin, 1971. Geological significants of Dezful embayment Boundaries. IOOC report No. 1166 (unpublished).

Petersen, S.A., B.A. Farrelly, and B. I. Braathen, 2003. Modelling of fluid effects in compartmentalized areas, an Oseberg south case study. EAGE 65th Conference and Exhibition, Stavanger.

Petersen, S.A., 2004. Optimization strategy for shared earth modelling. EAGE 66th Conference and Exhibition, Paris.

Petersen, S. A., 1999. Compound modelling, a geological approach to the construction of shared earth models. 61st Mtg. Eur. Assn. Geosci. Eng., 5012.

Rowbotham, P. S., and R. G. Pratt, 1997. Improved inversion through use of the null Space. Geophysics, 62, 869-883.

Santos, L., Schleicher, J., Tygel, M., and Tygel, M., 2000. Seismic modelling by Demigration. Geophysics, 65, 1281-1289.

Schmid, R., B. Link, and P. Butler, 1996. A comprehensive approach to depth imaging in thrust belt environments. 66th Ann. Internat. Mtg., Soc. Explor. Geophys., Expanded abstracts, 366-368.

Schneider, W., 1978. Integral formulation for migration in two and three dimensions. Geophysics, 73, 49-76.

Schultz, P. S., and J. W. C. Sherwood, 1980. Depth migration before stack. Geophysics, 45, 376-393.

Sepehr, M., 2000. The tectonic significance of Kazerun Fault zone, Zagros fold-thrust belt, Iran. Ph.D. thesis, Imperial College of London.

Sepehr, M. J. W. Cosgrov, 2004. Structural framework of the Zagros Fold-Thrust belt, Iran. Marine and Petroleum geology, 21, 829-843.

Sexton, P., and L. Lemaistre, 2004. Taking depth imaging further than flat image gathers. In: Estimation of accurate velocity macro models in complex structures. EAGE 66th Conference, Paris.

Sherkati, S., and J. Letouzey, 2004. Variation of structural style and basin evolution in the central Zagros (Izeh zone and Dezful Embayment), Iran. Marine and Petroleum Geology, 21, 535-554.

Slinger, F. C. P., and Crighton, J. G., 1959. The Geology and development of the Gachsaran field, southwest Iran. 5th World Pet. Cong. Proc. Sec. 1, paper 18, pp 349-375.

Soazig, Le B., H. Chauris, V. Devaux, S. Nguyen, and M. Noble, 2004. Velocity model estimation for depth imaging: Comparison of three tomography methods on a 2D real dataset. Geophysical prospecting, 52, 427-738.

Stork, C. and R.W. Clayton, 1991. Linear aspects of tomographic velocity analysis. Geophysics, 56, 483-495.

Stork, C. and R.W. Clayton, 1992. Using constraints to address the instabilities of automated prestack velocity analysis. Geophysics, 57, 404-419.

Stork, C., 1992. Reflection tomography in the post migrated domain. Geophysics, 57, 680-692.

Sukaramongkol, C., 1993. Seismic Imaging of a Non-Emergent Thrust Front In The Fallen Timber Creek Area, Southern Alberta Foothills. M.Sc. thesis, The University of Calgary, 140pp.

Suppe, J., 1983. Geometry and kinematics of fault-bend folding. Am. J. Science, 283, 684-721.

Thierry, P., G. Lambare, P.Podvin, and M.Noble, 1999. 3D preserved amplitude prestack depth migration on a workstation. Geophysics, 64, 222-229.

Treitel, S., and L. Lines, 2001. Past, present, and future of geophysical inversion-A new millennium analysis. Geophysics, 66, 21-24.

Van Trier, J., 1990. Tomographic determination of structural velocities from depth migrated seismic data. Ph.D. thesis, Stanford University.

Versteeg, R., 1994. The Marmousi experience: Velocity model determination on a synthetic complex data set. The Leading Edge, 13, 927-936.

Woodward, M., and U. Albertin, 2004. High-resolution velocity analysis in structurally complex areas. in: Estimation of accurate velocity macro models in complex structures, EAGE 66th Conference, Paris.

Xu, S., G. Lambare, and P. Thierry, 1999. 3D Migration/inversion in complex media. 69th Ann. Internat. Mtg., Soc. Explor. Geophys., Expanded abstracts.

Xu, S., and G. Lambare, 2004. Fast migration/inversion with multivalued ray fields: part1-Method, validation test, and application in 2D to Marmousi. Geophysics, vol. 69, 1311-1319.

Yan, L., and L. Lines, 2001. Seismic imaging and velocity analysis for an Alberta foothills seismic survey. Geophysics, 66, 721-732.

Yilmaz, O. 2001. Seismic data Analysis. Volume I: Society of Exploration Geophysicists.

Yilmaz, O., I. Tanir, and C. Gregory, 2000. A unified 3-D seismic workflow. Geophysics, 66, 1699-1713.